# Chapter 2 Binding studies of Anti-HBs, HBsAg, HCVAg and anti-T4 on solid phase

## 2.1 Introduction

The use of solid-phase systems in immunoassay are gaining popularity because virtually complete separation of the fractions can be achieved, particularly if washing protocols are included. Similarly, solid-phase assays are in general faster to perform and do not require extra time to form insoluble precipitates. Ideally, for the solid-phase approach to be acceptable in routine clinical chemical analysis, several criteria must be fulfilled. First, the solid-phase material chosen should be readily available and cheap. Second, the preparation and subsequent application of the adopted solid-phase system should not be more tedious in practice than the system which it intends to replace. Third, the solid phase should have high binding capacity and stability and low non-specific binding.

In an attempt to fulfill these criteria, a NR film solid phase was studied in detail with a view to provide a solid-phase suitable for use in a routine clinical chemistry laboratory. NR is produced locally and widely used in the manufacturing of biocompatible devices such as surgical gloves, urinary catheters, suctions tubes and so on. However it has not been used as a solid

phase for immunoassay though synthetic latex such as polystyrene latex is commonly used (Bernard,1986; Hiroko Kimura,1980). We find that natural rubber latex film has a high affinity toward protein and was selected as the solid support for the studies of anti-HBs, HBsAg and T4 assay. The molecules selected for the study covered a wide range of molecular size and composition, e.g. HBsAg, a lipoprotein, with molecular weight of 2.5-4.6 x $10^6$ daltons, anti-HBs a protein with molecular weight of 150,000 and T4 with molecular weight of 191.2. This will give a balance information on the surface properties of the new solid phase.

The spatial arrangement of proteins on the solid phase affects the sensitivity of the assay. For a better understanding of the underlying interaction between protein and surface, and their sensitivities, atomic force microscopy (AFM) and scanning electron microscopy (SEM) were used to study the organisation of the adsorbed molecules on the NR and PP surfaces.

AFM can be used to characterize surface chemical composition as well as the topography (Hansma et al., 1988; Burnham et al., 1990; Martin et al., 1987). AFM has recently become a method of choice to investigate 'soft' biological samples, eliminating the need for elaborate sample preparation techniques used in SEM and TEM. When AFM is used in the contact mode, the lateral force exerted by the tip results in image artifacts by disrupting the adsorbed proteins layer. The AFM imaging of known biological structures such as globular proteins and cyclic DNAs (Eppel et al., 1993; Bustamante et al.,

1992), demonstrates that the resolution of AFM imaging noticeably deteriorates due to physical contact of the probe tip with the object surface. Recently, a novel technique called tapping mode AFM (Digital Instruments) was developed which employs a silicon cantilever oscillating at a high amplitude. This mode largely avoids unfavorable tip/surface interaction encountered when using the contact mode and reduces the lateral force exerted on the sample. The advantages of imaging soft samples in the tapping mode include the absence of lateral forces that push aside weakly adsorbed molecules and smaller loading forces. Typically, when the AFM tip approaches the sample, the tip jumps to the sample at a critical distance due to van der Waals attraction. This mechanical instability sets a lower limit to the imaging force that can be used. This instability is circumvented in the tapping mode, and therefore, the only limit of the loading force is the accuracy of the electronics and detection system. Another important point when using AFM in contact mode is the variation of the loading forces resulting from induced drift of the cantilever. This effect is absent in the tapping mode, thus soft materials can be imaged at very low forces. Therefore tapping mode AFM was the technique chosen for this study, SEM was also used to characterize the sample at a submillimeter scale.

## 2.2 Materials and experimental methods

### 2.2.1 Materials and reagents

(a)The materials and reagents used for this study are summarised in Table A.

*Table A : Reagents and materials used*

| Reagent / Abbreviation | Source and/or formulation |
|---|---|
| High ammonia latex (HA) | Commercial product (Twice centrifuged) |
| Fetal calf serum, newborn (NBCS) | Paesel + Lorei GMBH & Co. Serile filtered, Art No 36-101-00003 |
| Sodium dihydrogen orthophosphate ($NaH_2PO_4$) | Ajax Chemicals. Sydney-Melbourne, Australia |
| Disodium hydrogen orthophosphate ($Na_2HPO_4$ ) | Ajax Chemicals. Sydney-Melbourne, Australia |
| Polypropylene tube (PP tube) | Abbot Laboratories, North Chicago, Cat.no.6171 USA. |
| HBsAg coating solution | Institute of Atomic Energy Beijing China - CIAE |
| Anti-HBs coating solution | Institute of Atomic Energy Beijing China - CIAE |
| HCVAg coating solution | Institute of Atomic Energy Beijing China - CIAE |
| $^{125}$I anti-human lgG | Institute of Atomic Energy Beijing China - CIAE |
| $^{125}$I HBsAg 203.5KBq | Institute of Atomic Energy Beijing China - CIAE |
| $^{125}$I anti-HBs 203.5KBq | Institute of atomic energy Beijing, China - CIAE |
| Positive control for HBsAg | In-house preparation (see text) |
| Negative control for Anti-HBs | In- house preparation (see text) |
| $^{125}$I Thyroxine ($^{125}$I T4) | Abbott RIA Tetrabead-125 T4 Diagnostic Kit (Solid phase) |
| Thyroxine standards (T4 Std) | Abbott RIA Tetrabead-125 T4 Diagnostic Kit (Solid phase) |
| Sheep anti-Thyroxine (anti-T4) | Guildlay , T010 |

**(b) Preparations of solution**

1. PBS (pH 7.4, 0.02M)

Phosphate buffer saline solution (PBS) was prepared by mixing 820 ml 0.04 M disodium hydrogen orthophosphate ($Na_2HPO_4$) and 180 ml 0.04 M sodium dihydrogen orthophosphate ( $NaH_2PO_4$ ) before the addition of 1000ml 280 mM sodium chloride solution and the resulting solution should have a pH of 7.4 and concentration of 0.02 M.

2.) Newborn Calf serum (NBCS)

NBCS was diluted to 50% (v/v) in PBS (pH 7.4) at room temperature.

3.) Anti-HBs, HBs Ag, HCVAg and anti-T4 coating solution

Frozen anti-HBs, HBsAg coating solutions were thawed and diluted in PBS pH 7.4. HCVAg was diluted in 0.05M pH 9.6 carbonate buffer. The total protein content in each of the coating solution was determined by the Lowry Method.

*Table B : Total protein content in each of the coating solution*

| Coating solution | Concentration (in neat sera)(mg/ml) |
|---|---|
| HBsAg | 0.176 |
| anti-HBs | 26.00 |
| HCVAg | 0.12 |
| anti-T4 | 27.60 |

4.) Positive and negative HBsAg / anti-HBs control sera

Anti-HBs positive controls sera were pooled from HBsAg negative patients. HBsAg positive control sera, HBsAg and anti-HBs negative control sera were gifts from the Blood Bank of University Hospital. Assays were carried out on the collected sera following IMK-441 system CIAE HBsAb SPRIA and IMK-413 system CIAE HBsAg SPRIA kit procedures based on coated polystyrene beads (as described below) .

i.) Procedure for coating anti-HBs and HBsAg on polystyrene beads

200µl of anti-HBs (or HBsAg) and 20 ml 0.02 M pH 7.4 PBS were mixed thoroughly in a beaker. 140 washed polystyrene beads of 0.79 cm diameter were added to the beaker. The beaker was agitated overnight on a table-top shaker at room temperature (26°C). The coating solution was discarded and the beads were washed four times with distilled water. 15 ml of 50% NBCS in 0.02M pH 7.4 PBS was added into the beaker to block the uncoated surface. Again the beaker was agitated on a table-top shaker at room temperature (26°C) overnight. NBCS was aspirated and the beads were washed four times with 0.02 M pH 7.4 PBS.

ii.)Assay procedure

300 µl of the pooled serum were incubated overnight with anti-HBs or HBsAg coated polystyrene beads in a polypropylene tube. These were then subjected to four washes with deionised water. The washed beads were allowed to react with 300 µl

of $^{125}I$ labelled anti-HBs or HBsAg and incubated at room temperature (26°C). The beads were further washed four times with distilled water and the bound radioactivites were counted in an Abbott Autologic Gamma Counter.

## 2.2.2 Experimental procedure

***Preparation of natural rubber solid phase***

100 µl of HA latex were pipetted into a polypropylene tube. They were rotated using a multi purpose rotator (model 150V, Scientific Industries INC) until the HA latex coated tube was completely dried. The NR solid phase thus prepared was then left at room temperature (26°C) to dry for 1 week before being immobilised with antibody or antigen. The area covered was sufficient to contain 200 µl of reactant.

**a.) Anti-HBs and HBsAg binding studies**

***(I.) Binding of $^{125}I$ anti-HBs & $^{125}I$ HBsAg on solid phase***

(i) 200 µl $^{125}I$ anti-HBs ( or $^{125}I$ HBsAg) were added to the NR coated tube. After incubation for 18 hours at 4°C, radioactivity was determined using Abbot Autologic Gamma Counter before and after washing ( four times with 1 ml of distilled water). The incubation steps were repeated for polypropylene tubes.

(ii) 200 µl of $^{125}I$ anti-HBs (or $^{125}I$ HBsAg) were dispensed into NR coated tubes and polypropylene tubes respectively. The binding was allowed to continue at 45°C

for various periods of time up to 30 hours. After incubation, the tubes were quickly washed four times with 1 ml distilled water. The activities of bound $^{125}I$ anti-HBs or $^{125}I$ HBsAg were counted using an Abbot Autologic Gamma Counter. All experiments were carried out in triplicate.

***(2.)HBsAg and anti-HBs assays***

***i.)Immobilization of anti-HBs and HBsAg onto solid surface***

Each NR coated tube or polypropylene tube used as a control was coated with 200 µl of anti-HBs (260 µg/ml) (Horse polyclonal) and HBsAg (1.76 µg/ml) and was left overnight at 4°C. The solution was decanted and the tubes were washed four times with 1 ml distilled water. The NR surfaces used for immobilisation of HCV (1 µg/ml) and anti-T4 (27.6 mg/ml) have been washed five times each with 1 ml of 0.1M HCl followed by five times with 1 ml distilled water.

***ii.) Blocking process***

200 µl of 50% NBCS were added into each tube, the tubes were left overnight at 4°C. The solution was decanted and tubes were washed four times with 1 ml of pH 7.4, 0.02 M PBS solution.

***iii.)HBsAg and anti-HBs immunoradiometric assay procedure***

Anti-HBs (or HBsAg) coated tubes were allowed to react for 2 hours with 200 µl of HBsAg (or anti-HBs) positive or negative control serum at 45°C. The tubes

were washed four times with distilled water. 200 µl of $^{125}$I anti-HBs (or HBsAg) were then added into each tube and incubated for 2 hours at 45° C. The bound radioactivities were counted with an Abbott Autologic Gamma Counter after four washes with 1 ml of distilled water. Control tubes were also set up to determine the extent of non-specific binding of $^{125}$I anti-HBs or HBsAg without serum preincubation (in addition to the non-specific binding with serum preincubation). The total activity of 200 µl of $^{125}$I anti-HBs (or HBsAg) was also counted. The percent binding (%B) = (Bound radioactivity/Total radioactivity) x 100% was computed . All assays were performed in triplicates.

**b.) anti-T4 Binding studies (T4 assay)**

***i.)Immobilisation of anti T4***

Anti-T4 solutions (Neat antisera - 27.6 mg/ml with 0.1% Sodium Azide as preservative) were prepared by diluting 1:25 in PBS to give a concentration of 1.10 mg/ml. 100 µl of anti-T4 coating solution was dispensed into each tube and were left overnight at 4°C. The solution was decanted and the tubes were washed four times with 1 ml distilled water. The NR coated tube used was prewashed five times with 1 ml 0.1 M HCl followed by five washes with 1 ml of distilled water (WNR). (WNR = NR coated tube prewashed five times with 1 ml 0.1 M HCl followed by five washes with 1 ml of distilled water)

***ii.)Blocking Process***

200 µl of 50% NBCS were added into each tube, and left overnight at 4°C. The solution was decanted and tubes were washed four times with 1 ml PBS solution.

***iii.)T4 competitive Binder Ligand Assay Procedure***

10 µl of standards or PBS were pipetted into each anti-T4 coated tube. 100 µl $^{125}I$ thyroxine (0.24 µCi/ml) in acetate buffer with protein stabilizer and 0.025% ANS (8-anilino-1-napthalene sulphonic acid) were added into the tube. The mixtures were mixed vigorously and incubated at room temperature (26°C) on a rotator set at 190 rpm for (60 ± 5) min. The tubes were washed with 2 ml deionised water before the bound radioactivity was counted in an Abbott Autologic Gamma Counter.

**c.) HCVAg binding studies (anti-HCV assay)**

***i.)Immobilisation of HCVAg (Hepatitis C Virus)***

WNR coated tube or polypropylene tube as a control was coated with 200 µl of HCVAg (6µg/ml) /tube and left overnight at 4°C. The solution was decanted and the tubes were washed four times with 1 ml distilled water

***ii.)Blocking Process***

200 µl of 50% NBCS were added into each tube, and left overnight at 4°C. The solutions were decanted and tubes were washed four times with 1 ml PBS solution.

***iii.) HCV immunoradiometric Assay Procedure***

HCVAg coated tube was allowed to react for 0.5 hour at 45 °C with 200 µl of anti-HCV positive or negative control serum. The tubes were washed four times with 1 ml distilled water. 200 µl of $^{125}$I anti-human IgG were then added into each tube and incubated for 2 hours at 45° C. The radioactivities were counted with an Abbott Autologic Gamma Counter before and after four washes with 1 ml of distilled water. All assays were carried out in triplicates.

**d.) Scanning electron microscope**

A Philip 515 scanning electron microscope operating at an accelerating voltage of 8-15 kV was used for examining the protein-immobilised solid phase morphology. Samples were prepared as described in 2.22 (a)(2), (b) and (c) and allowed to dry in a desiccator for 1-2 weeks at room temperature (26°C) before being coated with a gold sputter coater.

**e.) Atomic Force Microscope**

AFM measurements were performed with a Nanoscope (III) system (Santa Barbera, CA, USA), which uses an optical lever to measure relative changes in tip position.

The instrument was operated in the tapping mode using silicone nitride ($Si_3N_4$) cantilevers (Nanoprobes, Digital Instruments Santa Barbera, CA). The tip diameter reported by manufacturer was about 200 μm. Image sizes ranged from 2 x 2 $\mu m^2$ to 10 x 10 $\mu m^2$ with 512 x 512 or 216 x 216 measurement points (pixels). In all cases the polymer structure remained stable to repeated scanning. Several images were obtained for each sample, and duplicate samples were prepared. Representative images are shown. Sample were prepared as described in 2.22(a)(2), (b) & (c).

## 2.3 Results

In the study of the percent binding of $^{125}I$ anti-HBs and $^{125}I$ HBsAg on different solid phases, the results showed that the percent binding of both macromolecules was higher on NR coated surface compared to PP tube (Table 2.1 a & b, Fig 2.1 a, b(i) & b (ii)). However the percent binding of $^{125}I$ anti HBs was higher on both PP and NR surfaces as compared to $^{125}I$ HBsAg incubated at 4°C and 45°C respectively (Table 2.1 a & b, Fig. 2.1a, b(i) & b (ii)). The degree of non-specific bindings of the solid phase immobilised with HBsAg or anti-HBs and blocked with 50% NBCS was studied as follows. The solid phase immobilised with anti-HBs and HBsAg was preincubated with positive or negative control sera for two hours at 45°C. The tube was then incubated with $^{125}I$ HBsAg or $^{125}I$ anti-HBs to form the sandwich. The labelled macromolecule was discarded and the solid phase was washed four times with 1 ml of distilled water. The bound radioactivities

were counted. Uncoated solid phase which showed higher percent binding of labelled macromolecules without serum preincubation (Table 2.1 a) also gave higher non-specific bindings (with or without preincubation with HBsAg or anti-HBs negative sera) after immobilisation with anti-HBs or HBsAg. Non-specific binding (NSB) was higher on NR surface as compared with PP surface (Table 2.1 c & d, Fig. 2.2 & 2.3). The non-specific binding of NR surface immobilised with anti-HBs or HBsAg can be reduced by incubation in negative control serum. However, with PP tube, non-specific binding with or without incubation in negative control serum showed no significant difference (Table 2.1 c & d, Fig. 2.2 & 2.3).

The results show that direct bindings of $^{125}$I HBsAg and $^{125}$I anti-HBs by NR coated tube (without protein immobilisation) were 3.75-times and 15-times respectively higher than those on PP tube (Table 2.1a., Fig. 2.1a). However with PP tube as a solid phase, a more sensitive assay system was obtained because of the lower non-specific binding and higher specific binding of HBsAg and anti-HBs (as shown by a higher a/b ratio & a-b values in Table 2.1c, 2.1d). It suggests that adsorption of polyclonal antibodies and antigens on NR surface resulted in certain conformational changes resulting in lower binding capacity of the immobilised molecules. The specific binding of $^{125}$I anti human IgG (in anti-HCV assay) was also higher on PP as compared to NR surfaces (Table 2.1e & Fig. 2.5). The non-specific binding was much higher compared to anti-HBs and HBsAg immobilised tubes except for NR coated tube immobilised with HCV without serum incubation. In

addition NSB on serum tube was higher compared to non-serum tube. This could be due to non-specific interaction between IgG in anti-HCV negative serum with $^{125}I$ anti IgG resulting in formation of IgG-anti-IgG complex on the solid phase.

Similarly for T4 competitive binding ligand assay, PP solid phase give greater displacement of labelled T4 with increasing concentration of T4 standard as compared with NR surface (Table 2.1f, Fig. 2.4).

**Table 2.1a Comparison between NR and PP solid phases as direct binder of $^{125}$I HBsAg and $^{125}$I anti-HBs**

200 µl of each labelled macromolecules were incubated overnight with the solid phase (unwashed) at 4° C. The bound radioactivities were counted with Abbott Autologic Gamma Counter after four washes with 1 ml of distilled water.

*The numbers indicated in all the tables are the mean of three determinations together with their standard errors.This applies to all the Tables in the Chapter.

| Solid phase | * Percent binding | |
|---|---|---|
| | $^{125}$I HBsAg | $^{125}$I anti-HBs |
| PP | 0.08±0.00 | 0.18±0.06 |
| Unwashed NR | 0.30±0.03 | 2.70±0.06 |

**Table 2.1b Percent binding of $^{125}$I HBsAg and $^{125}$I anti-HBs on different solid phases.**

200 µl of each labelled macromolecules were incubated overnight at different times interval (45°C) with the solid phase (unwashed). The bound radioactivities were counted in an Abbott Autologic Gamma Counter after four washes with 1 ml of distilled water.

| Time/h | Percent binding | | | |
|---|---|---|---|---|
| | $^{125}$I HBsAg | | $^{125}$I anti-HBs | |
| | PP | NR | PP | NR |
| 0.5 | 0.08±0.01 | 0.68±0.08 | 0.12±0.04 | 4.19±0.22 |
| 1.00 | 0.07±0.01 | 0.95±0.10 | 0.17±0.08 | 5.13±0.19 |
| 1.50 | 0.10±0.00 | 1.34±0.15 | 0.19±0.03 | 5.64±0.17 |
| 2.00 | 0.10±0.01 | 1.86±0.18 | 0.16±0.01 | 7.22±1.01 |
| 2.50 | 0.13±0.02 | 1.82±0.08 | 0.17±0.00 | 6.92±0.08 |
| 3.00 | 0.12±0.02 | 2.55±0.32 | 0.16±0.02 | 7.09±0.09 |
| 4.00 | 0.12±0.01 | 2.56±0.62 | 0.18±0.03 | 7.81±0.75 |
| 5.00 | 0.13±0.00 | 2.59±0.37 | 0.22±0.03 | 7.59±0.13 |
| 6.00 | 0.16±0.01 | 2.49±0.33 | 0.22±0.05 | 7.90±0.19 |
| 9.00 | 0.18±0.06 | 3.23±0.68 | 0.31±0.01 | 8.29±0.42 |
| 10.00 | 0.17±0.04 | 3.59±0.22 | 0.42±0.12 | 10.35±1.08 |
| 30.00 | 0.21±0.07 | 4.01±0.60 | 0.86±0.08 | 12.14±0.23 |

**Table 2.1c Comparison between NR and PP solid phases (HBsAg assay)**

NR coated tube (unwashed) immobilised with anti-HBs , blocked with 50% NBCS and pre incubated with HBsAg positive control serum or HBsAg negative control serum or without serum preincubation before $^{125}$I anti-HBs was added. The bound radioactivities were counted with Abbott Autologic Gamma Counter after four washes with 1 ml of distilled water.

| Solid phase | Percent binding | | | Specific binding | |
|---|---|---|---|---|---|
| | With HBsAg Positive serum (a) | With HBsAg Negative serum (b) | Without serum | a-b | a/b |
| PP | 3.00±0.37 | 0.08±0.05 | 0.19±0.04 | 2.92 | 37.50 |
| NR | 2.66±0.03 | 2.05±0.07 | 2.73±0.13 | 0.61 | 1.30 |

**Table 2.1d Comparison between NR and PP solid phases (anti-HBs assay)**
NR coated tube (unwashed) immobilised with HBsAg and blocked with 50% NBCS and preincubated with anti-HBs positive control serum or anti-HBs negative control serum or without serum preincubation before $^{125}$I HBsAg was added. The bound radioactivities were counted with Abbott Autologic Gamma Counter after four washes with 1 ml of distilled water.

| | Percent binding | | | Specific binding % | |
|---|---|---|---|---|---|
| Solid phase | With anti-HBs Positive serum (a) | With anti-HBs Negative serum (b) | Without serum | a-b | a/b |
| PP | 4.33±0.26 | 0.07±0.02 | 0.07±0.02 | 4.26 | 61.86 |
| NR | 0.61±0.15 | 0.21±0.03 | 0.27±0.02 | 0.40 | 2.9 |

**Table 2.1e Comparison between NR and PP solid phases (anti-HCV assay)**
WNR coated tube immobilised with HCVAg and blocked with 50% NBCS and preincubated in anti-HCV positive control serum or anti-HCV negative control or without serum preincubation before $^{125}$I anti-human IgG was added. The bound radioactivities were counted with Abbott Autologic Gamma Counter after four washes with 1 ml of distilled water. WNR = NR coated tube prewashed five times with 1 ml 0.1M HCl followed by five washes with 1 ml of distilled water.

| | Percent binding | | | Specific binding % | |
|---|---|---|---|---|---|
| Solid phase | With anti-HCV Positive serum (a) | With anti-HCV Negative serum (b) | Without serum | a-b | a/b |
| PP | 2.38±0.02 | 1.45±0.01 | 0.28±0.02 | 0.93 | 1.64 |
| NR | 3.55±0.03 | 2.60±0.13 | 1.28±0.12 | 0.95 | 1.37 |

**Table 2.1f Percent binding of T4 on PP and NR surface**
NR and PP tube immobilised with anti T4 ( concentration = 1.1 mg/ml). It was then blocked with 50% NBCS. 100 µl of $^{125}$ I T4 and 10 µl of standard T4 were incubated at room temperature while rotating at 190 rpm for 60 min. The bound radioactivities were counted with Abbott Autologic Gamma Counter after four washes with 1 ml of distilled water.

| | Counts per minute | |
|---|---|---|
| Standard (µg/µl) | NR | PP |
| 0 | 8.14±0.44 | 13.60±0.15 |
| 3 | 6.00±0.17 | 9.71±0.68 |
| 6 | 3.24±0.13 | 4.86±0.01 |
| 12 | 2.36±0.10 | 2.54±0.05 |
| 24 | 2.02±0.06 | 2.33±0.02 |

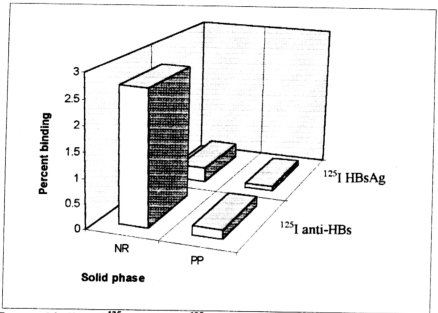


**Fig. 2.1a Percent binding of $^{125}$I HBsAg & $^{125}$I anti-HBs on solid phases**
200 µl of labelled macromolecules incubated overnight at 4°C on different solid phases, the supernatant was discarded. The bound radioactivities were counted with Abbott Autologic Gamma Counter after four washes with 1 ml of distilled water.

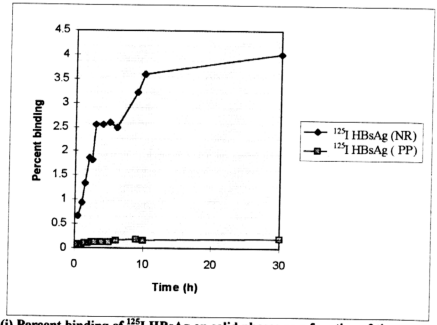


**Fig. 2.1b (i) Percent binding of $^{125}$I HBsAg on solid phases as a function of time.**
200µl of labelled protein incubated on different solid phases at 45° C for different times interval. The bound radioactivities were counted in an Abbott Autologic Gamma Counter after four washes with 1 ml of distilled water.

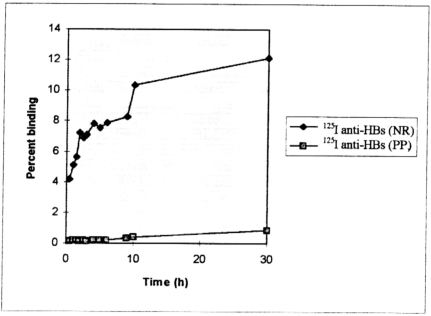


**Fig. 2.1b(ii) Percent binding of $^{125}$I anti-HBs on solid phases as a function of time.**
200 µl of labelled protein incubated on different solid phases at 45° C at different times interval , it was then discarded and washed four times with 1 ml of distilled water. The bound radioactivities were counted in an Abbott Autologic Gamma Counter.

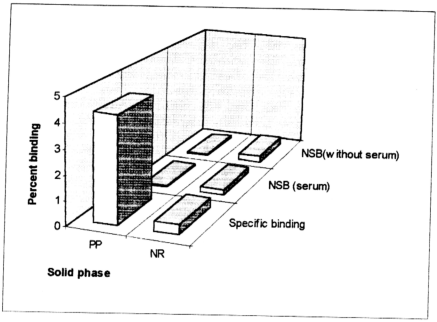


**Fig. 2.2. Comparison of $^{125}I$ HBsAg binding by NR coated and PP tubes in anti-HBs assay.** NR (unwashed) and PP surface immobilised with HBsAg, blocked with 50% NBCS then preincubated with anti-HBsAg positive control serum, anti-HBsAg negative control serum or without serum. The bound radioactivities were counted in an Abbott Autologic Gamma Counter after four washes with 1 ml of distilled water. Specific binding = Subtraction of percent binding in negative control serum from percent binding in positive control serum; NSB (serum) - non specific binding with negative control serum; NSB (without serum) - non-specific binding without serum preincubation.

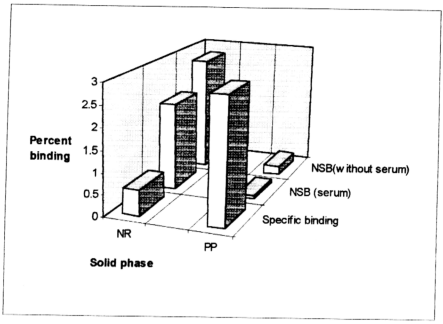


**Fig. 2.3. Comparison of $^{125}$I anti-HBs binding by NR coated and PP tubes, in HBsAg assay.** NR(unwashed) and PP surface immobilised with anti-HBs and blocked with 50% NBCS then preincubated with HBsAg positive control serum, HBsAg negative control serum or without serum. The bound radioactivities were counted in Abbott Autologic Gamma Counter after four washes with 1 ml of distilled Water. Specific binding - Subtraction of percent binding in negative serum from percent binding in positive control serum; NSB(serum) - non specific binding with negative control serum; NSB (without serum) - non-specific binding without serum preincubation

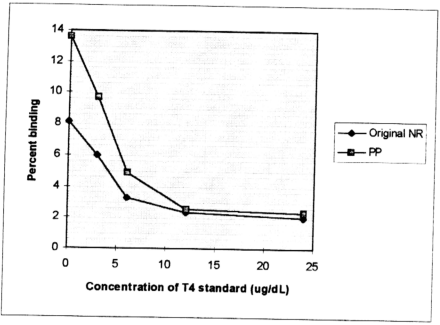


**Fig. 2.4 Comparison of $^{125}I$ anti-T4 percent binding on NR coated and PP tubes**
Solid phase (NR and PP) immobilised with anti T4 at a concentration of 1.1 mg/ml, and blocked with 50% NBCS. 100 µl of $^{125}I$ T4 and 10 µl of standard T4 were added and incubated at room temperature while rotating at 190 rpm for 60 min. The bound radioactivities were counted in Abbott Autologic Gamma Counter after four washes with 1 ml of distilled water.

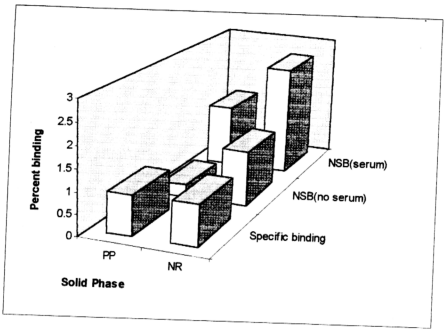


**Fig. 2.5. Comparison of $^{125}$I anti-Human IgG binding between NR coated and PP tubes, for anti-HCV assay.**

Solid phases ( WNR and PP) immobilised with anti-HBs and blocked with 50% NBCS then preincubated with positive anti-HCV serum, negative anti-HCV serum or without serum. The bound radioactivities were counted in Abbott Autologic Gamma Counter after four washes with 1 ml of distilled water. Specific binding = Subtraction of percent binding in negative control serum from percent binding in positive control serum; NSB (no serum) - Non specific binding without serum incubation; NSB (serum) - Non specific binding (with negative control serum)

WNR = NR coated tube prewashed five times with 1 ml 0.1M HCl followed by five washes with 1 ml of distilled water.

## 2.4 Discussion

### 2.4.1 General discussion

Three forms of HBsAg in sera of patients with acute or chronic hepatitis B infection can be detected by antibody directed against HBsAg. The predominant form observed by immune electron microscopy consists of 18-22 nm diameter spherical particles while smaller amounts of variably long filamentous particles of the same diameter were also present (Bayer et al., 1977) [Fig 2.6(a)&(b)]. Many HBsAg positive sera also possess larger spherical or Dane particles in much smaller concentrations (Dane et al., 1970). These are 42 nm in diameter, with an outer envelope (having HBsAg reactivity) and an inner core, or nucleoside (having HBcAg reactivity) which are antigenically distinct (Almeida et al., 1969)( Fig 2.6(b)). HBsAg also contains host lipid and possibly host serum or hepatocyte cell surface proteins and /or glycoproteins (Blumberg et al 1967., Howard et al., 1976). In addition the electron dense inner core (HBcAg) of the Dane particle is approximately 28 nm in diameter (Fig 2.6(c)). It consists of several protein components of distinct molecular weight (Fields et al., 1977) and a small circular, partially double stranded DNA molecule which is $1.6x10^6$ daltons in size (Robinson, 1977) It also has associated DNA polymerase activity (Hirschman, 1979) and possesses a serologically defined e antigen (HBeAg) activity (Fig 2.6(d))

**Figure 2.6. The major serum forms associated with HBV infection** ( Feitelson 1985)

Electron micrographs of (a)22 nm small spherical HBsAg particles; (b) variably long filamentous HBsAg particles. (Bars indicate 100 nm) (c) Intact Dane particles (d) Diagrammatic representation of serum derived particles from infected patients.

(a)

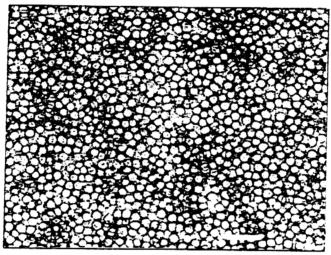

(b)

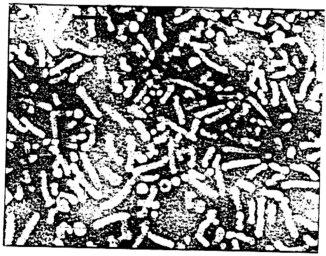

(c)

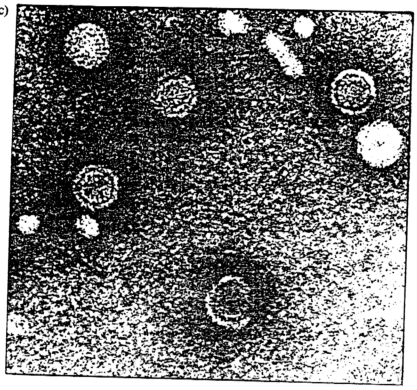

(d)

1. HBsAg: Particles with HBsAg (a.d/y, w/r)
2. HBcAg Dane particle core with HBcAg on its surface and DNA polymerase activity
3. DNA and DNA polymerase : Circular, double stranded Dane particle DNA with a single stranded gap up to 1/3 of circle length. DNA polymerase reaction makes the single stranded region double stranded. Molecular weight of circular, double stranded Dane particle DNA = $2.0 \times 10^6$ daltons. HBeAg : $3 \times 10^5$ dalton protein antigenically and physically distinct from HBsAg and HBcAg ( Feitelson, 1985)

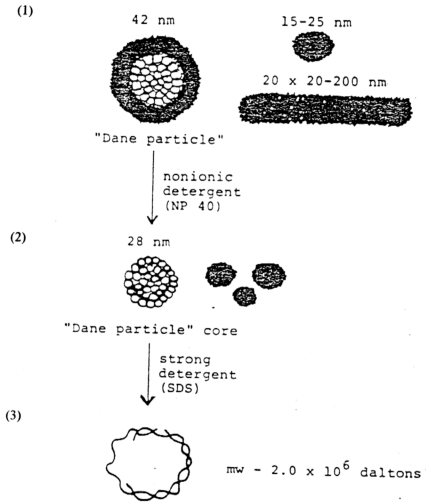

The association of serum components with 22 nm size spherical HBsAg particles, and repeated attempts to purify HBsAg free from these components, have resulted in only partial agreement as to the physical and chemical properties of these HBV (Hepatitis B virus) associated forms (Howard,1976). Table 2.2 below shows some properties of the spherical HBsAg particles.

*Table 2.2 . Some physical and chemical properties of the spherical 22 nm HBsAg particles*

| Parameter measured | Result | References |
|---|---|---|
| 1. Particle diameter | 16-25 nm | Almeida et al., 1969 |
| 2. Particle molecular weight | 2.5-4.6 x $10^6$ Daltons | Skinhoj et al., 1973 |
| 3. Particle density | 1.20-1.27 gm/ml | Neurath et al., 1981 |
| 4. Particle isoelectric points | pH 3.6- 5.7 | Howard et al., 1977 |
| 5. alpha helical content | 70-80% | Shih et al., 1980 |
| 6. Total protein content | 40-70% | Howard et al., 1976 |
| 7. Total carbohydrate content | 3.6-6.5% | Chairez et al., 1973 |
| 8. Total lipids | 22.54% | Neurath, 1982 |

The anti-HBs used for immobilisation were horse polyclonal IgG antibodies and the anti-HBs used for labelling with $^{125}$Iodine were mouse monoclonal antibodies. IgG is a hybrid molecule and consists of four separate polypeptide chains: two of these have about 440 amino acids, called heavy chains, and two possess 220 amino acids called the light chains. Molecular weight of IgG is 150,000 which is in monomeric form. It contains not only amino acids but also small amount of carbohydrates (2.6%)(Turner, 1977)

Thus, both the HBsAg and anti-HBs used contain mostly protein with small amount of carbohydrate and lipid. The proteins are macromolecules consisting of some 20-30 different L-amino acids which are linked to each other forming a linear

polypeptide chain. Many proteins consist of only a single polypeptide chain; others contain two or more chains which may be identical or different. Two ( $\psi$ and $\phi$ ) of the bonds in the peptide unit are, in principle, free to rotate. The C-N bond, which is shaded in Fig 2.7, is rigid because of its partial double bond character. Some side-chains are acidic, others are basic, thus rendering the polypeptide amphoteric. Side-chains vary in hydrophobicity (polarity), making the polypeptide chain amphiphilic as well.

**Fig. 2.7 Structure of a peptide in a polypeptide chain. Two ( Ψ and Φ ) of the three (backbone) bonds are free to rotate; the shaded bond is rigid. R and R' represent amino acid side-groups.**

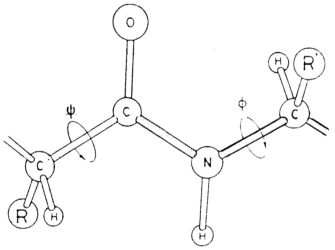


Three-dimensional structures of proteins may be broadly classified into (a) molecules that are highly solvated and flexible, resulting in an expanded (but rarely random) coil structure; (b) molecules that have adopted a regular structure like an α-helix or a β-pleated sheet called the fibrous proteins; and (c) densely packed

molecules of roughly spherical shape containing a considerable amount and variety of internal architecture known as the globular proteins. Small spherical HBsAg particle show a highly compact physical structure with remarkable antigenic structure and 70-80% of the proteins are alpha-helical in nature. Most of the activity of proteins in HBsAg are of the type (b) & (c) whereas anti-HBs which are immunological proteins are mainly globular protein. For proteins belonging to classes (b) and (c) mentioned above, the conformation of the polypeptide backbone is more or less fixed.

Globular proteins in an aqueous environment have a number of structural characteristics in common (Haynes & Norde, 1994):

i.) They are more or less spherical, with molecular dimensions in the range of 10 to 100 nanometers.

ii.) Hydrophobic side-groups tend to be buried in the interior of the molecule where they are shielded from contact with water. As a result, part of the hydrophilic hydrogen-bond-forming polypeptide backbone must also be located in the interior. Therefore one important property of secondary structures such as α-helices and β-sheets is the efficient matching of hydrogen bond donors and acceptors between the internal polar groups of the polypeptide backbone. However from computer graphic images of native bovine pancreas ribonuclease (Rnase) (Haynes & Norde, 1994), other structural characteristics beyond those listed above are apparent in these images. First, not all hydrophobic residues are hidden in the interior. Second, polar and non-polar residues are more or less evenly distributed over the protein surface;

surface; no regions are observed where the surface shows either a distinctly hydrophilic or hydrophobic character (Haynes & Norde, 1994).

iii) Charged groups are always located in the aqueous periphery of the protein. Any charged groups in the interior occur as ion pairs since dissociation is strongly opposed by the low local dielectric permittivity.

iv) The atoms are closely packed, with most adjacent atoms in van der Waals contact. Internal atomic packing densities average 75%, which is similar to the maximum packing density of equal-sizes hard spheres. Thus short range interactions such as van der Waals and hydrogen bonding can play important role in stabilization of folded protein.

### 2.4.2 Driving forces of antigen and antibody adsorption at NR and PP solid phases

HBsAg and anti-HBs which are α-helices and β-pleated, globular proteins are extremely compact. Their free volumes, compressibilities, and conformational freedom are comparable to those in glasses and polymer crystals (Dill, 1990). Such a compact inflexible architecture is possible only if interactions within the protein molecule and between the protein molecules and its environment are sufficiently favourable to compensate for the substantial loss of conformational entropy.

Adsorption of protein on solid surface is a complicated process because it is determined by a delicate balance between several attractive and repulsive interactions. The relative importance of the various 'driving forces' is different for

various classes of proteins and also depends on the solid surfaces. However interactions that determine the adsorption of HBsAg or anti-HBs on both PP surface and NR surface can be divided into three categories:

**(i) Protein-surface interactions**

These interactions can have various origins such as electrostatic attraction or repulsion between the protein. The fundamental structure of the natural rubber isolated from the *Hevea brasiliensis* tree has been shown to consist of an initiating terminal group, two or three trans-isoprene units, a long sequence of cis-polyisoprene unit and a terminal group aligned in that order ( Tanaka, 1989). Both natural rubber and polypropylene surfaces are hydrophobic. Such materials are electrically neutral and ionic mechanism of adsorption would not be expected. However plateau value for protein adsorption often shows a maximum at the isoelectric point (IEP) of the protein/sorbent complex. This implies that coulombic interactions due to net charge of the protein and surface influence the adsorption behavior. At pH 7.4, both HBsAg and anti-HBs possess net negative charges resulting from the dissociation of various amino acids located mostly on the periphery of the molecules. Moreover natural rubber latex particles are amphoteric in nature with an isoelectric point of pH 3.8 (Ho et al., 1976). Any non-homogeneity in the charge distribution, the so called 'mosaic charge distribution', can lead to a dipole moment contributing to electrostatic interaction. Protein adsorption results in a complex overlap of electric fields which involves charge interactions between protein and sorbent, between adjacent protein molecules, ion

pairing between oppositely charged groups on the protein and sorbent surface, redistribution of protons in the aqueous phase and on the surface of adsorbed protein molecules, reduction in the dielectric constant of the interfacial layer, and consequently, coadsorption of low molecular weight counterions to neutralize excess charge in the interfacial region.

**(ii) Dehydration of interface on the outside of the protein and on the solid surface**

All proteins, α-helix or β pleated-sheet, regardless of their native-state stabilities and electrokinetic charges, adsorb to some extent on hydrophobic surface. Dehydration of hydrophobic interface promotes protein adsorption. Since both HBsAg (16-25 nm) and anti-HBs have large radii compared to that of a water molecule (0.14 nm), adsorption results in the displacement of a large number of water molecules. The sign of dehydration effect is a large decrease in total heat capacity, which is usually observed in protein adsorption processes where the sorbent surface is hydrophobic. Dehydration of hydrophobic surface results in an entropy gain of 20-50 $\mu J\ K^{-1}\ m^{-2}$ (Haynes & Norde, 1994) which alone can easily drive spontaneous protein adsorption. Therefore this interaction is very important and often predominates over the other driving forces. Under most conditions, the contribution of dehydration of a hydrophobic surface to the overall Gibbs energy(G) of adsorption is much larger than that of electrostatic interaction between the protein and the sorbent (Norde and Lyklema, 1991). Studies by Buijs (1995), on

both positively and negatively charged hydrophobic surfaces had shown that the affinity of the proteins for the hydrophobic lattices was barely influenced by electrostatic interactions. However, at saturation level the adsorbed amounts were dependent on the overall electrostatic interactions resulting in a maximum amount adsorbed when the protein charge was partly compensated by the sorbent surface charge.

**(iii) Structural changes in the protein molecule upon adsorption**

The densely folded structure of anti-HBs or HBsAg proteins in solution is attributed mainly to the fact that hydrophobic interactions in the interior of the molecule (i.e., prevention of hydration of these residues) are stronger than the intramolecular electrostatic repulsion in the periphery of the molecule and the loss of entropy upon folding. The importance of the hydrophobic effect in protein folding and adaptability was first recognised by Kauzmann who reasoned that protein folding is driven by a large entropy gain in the solvent molecules released from hydrophobic residues during the folding process (Kauzmann, 1959). Thus, the existence of compact globular proteins in solution is an illustration of the constructive power of chaos : the ordered protein structure is preferred. However when the protein is brought into contact with a hydrophobic interface the balance between these forces may change because the hydrophobic interior of the molecule can avoid hydration in an alternative way by positioning itself against the interface. Thus adsorption of proteins to solid surfaces (particularly hydrophobic surfaces)

may involve the formation of a water-free contact layer where the protein can unfold without solvating all its hydrophobic residues. This unfolding can be promoted by electrostatic repulsion between the charges on the adsorbed protein. Based on calorimetry data for single domains proteins, an entropy (S) gain between 1.4 and 2.9 kJ $K^{-1}$ per mole of protein is expected for the adsorption of a 100-residue globular protein. This gain in entropy would contribute between -420 and -900 kJ per mole of adsorbed protein to the driving force for adsorption at 300K. Moreover it was also observed that the folded conformation of the globular protein is only marginally stable. For single domain protein, maximum values for $_{N\text{-}G}$ G (i.e., maximum native state stabilities) ( $_{N\text{-}G}$ G = Gibbs energy of denatured state - Gibbs energy of folded state) are in the 20 to 100 kJ/mol range, roughly equivalent to the energy required to rupture 1-8 hydrogen bonds. This indicates that protein unfolding is a highly cooperative process; the disruption of any significant portion of the folded structure leads to unfolding of the rest. Unfolding of the adsorbed protein will increase the surface area occupied per protein molecule . That is unfolding of protein would cause the protein to be more evenly spread out as can be seen from SEM micrograph (Fig 2.10 - 2.11). Protein unfolding is actually referred to as the structural transition from globular state or α-helix or β-pleated-sheet, the native state (c) to the denatured state (a). It will also reduce the electrostatic repulsion between the like charges in the adsorbed immobilised protein because these become more distant, and increase the entropy of the protein.

There is now substantial evidence that solid/water interfaces can upset this delicate balance by providing a region on which the polypeptide backbone can unfold without exposing hydrophobic residues to the water molecules. Evidence for rearrangements in protein structure upon adsorption have come from transmission circular dichroism, NMR and fluorescence spectroscopies, and protein titration data. The most convincing evidence has come from micro-DSC (Differential scanning microcalorimetry) experiments which indicate that most of the ordered secondary structure in native globular proteins is lost when the proteins adsorbed onto negatively charged polystyrene ( a moderately hydrophobic surface) surface (Haynes & Norde, 1994).

Additional proof that structural rearrangements in protein molecule provide a strong driving force for adsorption lies in the general tendency for proteins with low native-state stabilities to adsorb under seemingly unfavourable conditions where, for instance, the surface is hydrophilic and / or the protein and the sorbent surface carry the same charge sign. Examples include the adsorption of lactalbumin (LA) and Bovine serum albumin (BSA) on glass and $\alpha$-$Fe_2O_3$. Studies also showed that IgG was adsorbed onto hydrophilic surface even under conditions of electrostatic repulsion (Suzawa & Shirahama, 1992; Elgersma & Zsom, 1992). In these experiment, adsorption cannot be driven by sorbent-surface dehydration or global electrostatic effects. Hence, some other factors must favour the adsorption process to an extent that outweighs the opposition from hydrophilic dehydration and electrostatic repulsion. It is plausible to relate this additional driving force to

structural rearrangements in the protein molecule. As shown by Norde and Favier (1992), both BSA and hen's egg lysozyme (LSZ) undergo structural alterations upon adsorption at the hydrophilic silica surface with the same charges and the effect diminishes with increasing coverage of the sorbent surface by the protein. A reduction of the helical structure is seen. It is therefore likely that conformational entropy production drives the adsorption process in these systems. Thus adsorption of anti-HBs and HBsAg on electrostatically repelling NR surface ( both are negatively charge under these conditions) may have undergone structural changes too.

**2.4.3 Immobilisation of antigen and antibody on PP and NR surface**

Total percent bindings of both labelled macroproteins (antibody / antigens ) were much higher on NR surface than on PP tube. Proteins adsorbed differently on both surfaces. SEM micrographs show that macroproteins (antibody / antigens ) were adsorbed on PP surface uniformly but were as clusters on WNR surface as observed in WNR coated tubes immobilised with anti-T4 or HCVAg and unwashed NR coated tubes respectively (Fig 2.10-2.17). Some possible explanations for the above observations are :

(i) Labelled proteins may be trapped in the uneven surface of NR which result in high percent binding of protein.

(ii) Difference in hydrophobicity of the two surfaces affects the degree of unfolding or conformation of the adsorbed proteins.

(iii) Interactions of inorganic substances and proteins originated from the NR latex with the immobilised antibody/antigen proteins enhanced the formation of antigens and antibodies aggregate. The validity of each of these explanations is discussed below.

(i) SEM micrographs showed that both the PP and NR surfaces were flat and smooth (Fig 2.8). However AFM (Fig. 2.9) images show a clearer picture where NR surface was much rougher compared to the PP surface. Many protruding spherical particles were seen on the NR surface. High percent binding of labelled macromolecules immobilised on NR surface are thought to be the trapping of antigen or antibody molecules between the uneven areas of the NR surfaces. However by repeated washing, we found that only a small amount of adsorbed antigen and antibody proteins dissociated from the NR surface. After incubating for 48 hours and washing 30 times with 1 ml distilled water, the percentage of labelled protein ($^{125}$I anti-HBs and $^{125}$I HBsAg) immobilised on NR surface remained at 83.85% and 97.30% respectively (Table 3.2b(i)). Thus the decrease in percent binding on the NR surface are minimal even after washing. This shows that the proteins were firmly bound on NR surface and not trapped inside it. The amount of antibody/antigen protein adsorbed depends on the interrelation between a substrate and the protein. Antibody/antigen protein adsorption is affected easily by the surface characteristics of the substrate onto which adsorption occurs. We attribute the high percent binding on NR surface to its surface characteristics as explained below.

(ii)The extent of unfolding of a protein as mentioned above also depends on the characteristics of the substrate (Norde & Lyklema, 1991). A hydrophobic surface promotes unfolding, results in greater conformation change of the adsorbed proteins. The amount of protein adsorbed increases as the surface become more hydrophobic. Table 2.3 shows a list of studies which demonstrate this fact. Proteins immobilised on hydrophobic surface are irreversible and could not be displaced by other proteins.

*Table 2.3 Adsorption of proteins on difference surfaces*

| Solid phase/Treatment on solid phase | | Contact Angles | Protein | Phenomenon (Reference) |
|---|---|---|---|---|
| Silicon | 1. Hydrophilic silicon prepared by immersion in hot chromosulfuric acid<br><br>2. Hydrophobic silicon-silicon modified by dimetyldichlorosilane | Determined with bidistilled water<br>8.8 °<br><br>102° | BSA | Hydrophobization of the silicon surface resulted in a 58-fold increase and a 27-fold decrease of the adsorption and desorption rate constants of BSA as compared with the appropriate rate constant of a hydrophilic surface. The maximal surface concentration of BSA in PBS pH 7.4 on hydrophilic surface is 1.18 $mg/m^2$ , and on hydrophobic surface is 0.89 $mg/m^2$. Denaturation of BSA on the hydrophobic silicon surface is greater than that on the hydrophilic surface (Tautgirdas et al., 1992). |
| 1.Germanium<br>2. Poly(hydroxyethyl methacrylate)<br>3.Biomer (segmented polyether poly-urethane)<br>4. Polystyrene | | measured using a goniometer<br><br>19.3 °<br>35.5 °<br><br>37.6 °<br><br>90.5 ° | Fibrino-gen | The adsorption kinetics of fibrinogen from 1 mg/ml showed that the amount of adsorbed fibrinogen increased as the surface become more hydrophobic. The results also indicated that the adsorbed fibrinogen underwent a large degree of conformational changes as the surface hydrophobicity increased (Donghao et al., 1991) |
| Silica<br>Quartz | Silica Quartz (untreated)<br><br>Hydrophobic silica quartz - quartz were made hydrophobic by chemically modified with $C_{18}$ alkyl chain | measure by sessile drop technique<br>14 °<br><br>115 ° | Synthetic β - sheet forming peptide | Adsorption carried out over the same length of time resulted in greater surface coverage for the hydrophobic than for the hydrophilic, 0.393 and 0.138 $mg/m^2$ respectively. A comparison of the circular dichroism spectra of the β-peptide suggested that a conformational change had taken place upon adsorption compared to hydrophilic surface (Harvey et al., 1995). |

| Solid phase/Treatment on solid phase | | Contact Angles | Protein | Phenomenon (Reference) |
|---|---|---|---|---|
| Silica | Hydrophilic silica<br><br>Hydrophobic silica-methylated silica | <10°<br><br>95 (advancing)<br>88° (receding) | HSA, fibrinogen, IgG | Preadsorption of HSA on (hydrophobic) methylated silica effectively blocked further adsorption of fibrinogen and IgG due to an irreversible conformational change of HSA on these surfaces. On the other hand, hydrophilic silica displayed a (partial) displacement of preadsorbed HSA on addition of fibrinogen. The saturation amount of HSA adsorbed on silica and methylated silica are 0.35 mg $m^{-2}$, 0.80 mg $m^{-2}$ ; for fibrinogen the corresponding amounts are 2.9 mg $m^{-2}$ and 4.9 mg $m^{-2}$; those for IgG are 1.1 mg $m^{-2}$ and 3.0 mg $m^{-2}$ (Malmsten & Lassen,1995) |
| Silica | Hydrophilic silica<br><br>Hydrophobic silica -Silica modified with aminoalkyl (decylamine) and thioalkyl(butanethiol) | 16.8°<br><br>69°<br><br>46.9° | HSA, IgG | Upon increasing the chain length of the thioalkyl-derivatives from 4 to 10, binding capacity of HSA increase, when nitrogen is replaced by sulphur in buthylamine, the binding capacity of HSA diminished by four times.<br>The hydrophobic decylamine and decylcaptan-derivatised silica show decreased binding capacity of IgG when covered with HSA, but the capacity to bind IgG to underivatised silica covered with HSA increased slightly (Oscarsson, 1994) |
| Glass | | | HSA, fibrinogen | Fibrinogen displaced HSA to a large extent (Norde,1986) |

A number of parameters have been used to establish relative hydrophobicities of solid surfaces, the most common are the contact angle of water , the Gibbs energy (or reversible work ) of hydration and surface tension of the solid surface. The surface tensions for NR surface and polypropylene, Teflon and glass which may be classified as most hydrophobic and hydrophilic are shown in Table 2.4.

*Table 2.4 Comparison of solid surface tension characterising the hydrophobicity of solid surfaces in aqueous solution*

| Surface | ($mJm^{-2}$) |
|---|---|
| Polypropylene[a] | 25.7 |
| Synthetic polyisoprene[b] | 24.1-29.6 |
| Natural rubber[b] | 28.7-31.4 |
| Glass[c] | 138.0 |
| Teflon[a] | 18.0 |

[a] Data taken from ( Oss, 1991)
[b] Data taken from (Ho & Khew, 1996 )
c Data taken from (Sjollema, 1990)

Data show that NR surface is slightly more hydrophilic than polypropylene tube (Table 2.4). The protein-substrate interactions will be more favourable if the hydrophobic or non-polar surface domains of the protein molecule are not in contact with water. This would result in an orientation of the hydrophobic domains towards the substrate surface, thus promoting unfolding and more homogeneous coverage of the surface as revealed by electron micrograph (Fig. 2.10(a) - 2.12(a)). HBsAg and anti-HBs are adsorbed as aggregates on WNR surface (Fig. 2.14(a),(b) & 2.15(a),(b)) This may be the result of the less hydrophobic NR surface causing the adsorbed molecules not to unfold. Thus it is more favourable for the hydrophobic regions of the protein to bury inside the adsorbed layer resulting in less unfolding of the protein compared to PP surface (Fig. 2.14 - 2.17). However it has been shown previously that the degree of adsorption of hydrophilic proteins (i.e. soluble proteins, at pH values significantly below or above their isoelectric points), at low concentrations, onto hydrophobic surfaces was roughly ten times greater than their

adsorption on hydrophilic surfaces (MacRitchie, 1972.) The reverse was observed here. One possible reason may be due to the formation of clusters of protein.

iii.) All proteins adsorbed on NR surface appeared in clusters. A hydrophilic surface would decrease the extent of conformation change of adsorbed protein but would not result in the formation of aggregates or clusters. Interaction of the natural rubber surface with immobilised proteins will enhance the formation of aggregates. For examples addition of divalent ions $Ca^{2+}$ to protein samples at low concentration enhanced aggregation. However aggregation of proteins may occur before the adsorption process. Further investigations are needed to confirm this (Klotz, 1993).

Our results show that the percentage binding of labelled anti-HBs was generally higher than that of the labelled HBsAg on uncoated PP and NR surfaces. However electron micrographs show HBsAg occupied a larger surface area compared with anti-HBs. The molecular weight of HBsAg is 2.4 - 4.6 $x10^6$ Daltons and the molecular weight of the $^{125}I$ labelled IgG monoclonal antibody is 150,000 Daltons. Thus van der Waals attraction of HBsAg by the surface is expected to be greater and as the molecule unfolds, it will occupy more space, thus the number of $^{125}I$ labelled HBsAg molecules bound onto the surface is lower and therefore less binding of $^{125}I$ labelled HBsAg ( one molecule of HBsAg is usually labelled with one atom of $^{125}Iodine$). The adsorbed mass correlates reasonably well with the molecular size, i.e., the larger the molecular size, the more mass adsorbed on a given surface. This is in agreement with results of previous work (Suttiprasit, et al,

1992). In particular, a large molecular weight (large size) would suggest availability of a large number of potential non-covalent contacts with the surface.

### 2.4.4 Assay of immobilised antigen and antibody on uncoated PP and NR surface

The present results showed that, $^{125}I$ labelled HBsAg and labelled anti-HBs bound 3.5-times and 15-times ( Fig. 2.1) more on NR coated tube as compared to PP tube. However with PP tube as solid surface, more sensitive assay was obtained with low non-specific bindings and high specific binding (Fig. 2.2 & 2.3). Some possible explanations are:

(i) Polyclonal antibodies and antigen passively adsorbed on NR coated surface had undergone substantial conformational changes (by aggregation) to drastically affect their binding capacity (the paratope of anti-HBs and epitope of HBsAg are hidden). Most of the immobilised antibodies or antigen on NR surface are inactive in its binding properties. Previous experiments have indicated that passive adsorption of protein resulted in molecular alterations which in turn can alter their functions. Table 2.5 lists some of these studies.

*Table 2.5 Conformational changes on proteins adsorption*

| Protein | Phenomenon | Reference |
|---|---|---|
| Albumin | Conformational changes after adsorption on glass | Bull, 1956 |
| IgG | Molecular unfolding and change in antigenicity when adsorbed on polystyrene | Kochwa et al.,1967 |
| IgG | Thermodynamic evidence for conformational change | Nyilas et al., 1974 |
| Monoclonal Ab | Altered specificity after adsorption | Kennel., 1982 |
| Tryptophan synthase | Alter enzymic and antigenic activity after adsorption | Djavadi-Ohaniance et al., 1984 |
| Lactic dehydrogenase | Conformational alteration after adsorption on polystyrene | Holland and Katchalski-Katzir; 1986; Friquet et al., 1984 |
| Monoclonal Ab | Loss of activity after adsorption on polystyrene | Suter and Butler, 1986 |
| IgG,IgA | Loss of antigenicity after adsorption on polystyrene | Dierks et al., 1986 |
| Ferritin | Cluster formation on silica wafers | Nygren, 1988 |

However can the type of solid phase used affect the degree of denaturation of the adsorbed antibody/antigen proteins ? Or is it the intrinsic property of a captured antibody? There have been few attempts to visualize the adsorbed proteins. Nygren (1988) & Feng et al., (1989) found that fibrinogen appeared in cluster form as it was adsorbed on to graphite. These investigators found that albumin adsorbed onto the same surface showed little aggregation or denaturation. However it has been observed that (Joshi et al., 1992) some adsorbed polyclonal captured antibodies [Polyclonal mouse anti-fluorescein (anti-Flu)] had lower affinity on polystyrene surface than when immobilized using protein avidin capture system (PABC). The loss of functional activity due to immobilization of monoclonal captured antibodies (Cabs) by passive adsorption, can be minimised by immobilisation the captured antibodies via an antiglobulin or a streptavidin bridge (Butler et al., 1992). This resulted in the preservation of greater than 70% antibody binding sites for some

monoclonals (Butler et al., 1993). It was concluded that any form of immobilisation was accompanied by loss of binding but the use of different solid phases resulted in different degree of denaturation. Butler found no difference in the performance of anti-Flu Cabs (Captured antibodies) adsorbed on Immulon 2 versus Maxisorp from NUNC, while anti-Flu Cabs adsorbed on both of these surfaces performed slightly better than when adsorbed on NUNC Polysorp and significantly better than when adsorbed on polyvinyl plates. (Butler et al., 1991,1993). Thus the binding characteristics of adsorbed protein was affected by the surface characteristics of adsorbent (Oscarsson, 1994).

(ii)The SEM micrographs and AFM pictures (Fig. 2.10-2.13) show that HBsAg, anti-HBs, HCVAg and anti-T4 were evenly coated on polypropylene surface due to the flattening of the protein molecules upon adsorption. The shape of the aggregate of anti-HBs on PP (Fig. 2.11) surface changed from branched to thread like structure, while some areas were completely covered with dendrite-like aggregates. HBsAg on PP (Fig. 2.10) surface showed a much denser coating which covered almost the whole surface at certain areas. In addition, nucleation of high density islands superimposing on thin layer coverage of HBsAg was observed. T4 on PP surface displayed thin fibrils connected to large globular structures. Circular areas varying from 1.5 to 5μm (Fig. 2.12a(i)) in diameter with thick centered-oriented aggregates were distributed with areas of thin fibrils in between them. The difference in protein organisation was apparent in terms of fibril thickness and the distances between the fibrils. Besides each large globular structure was surrounded

by isolated smaller spherical structure, possibly molecules. On NR surface (Fig. 2.14-2.17), the proteins were randomly distributed in clusters. Aggregates of HBsAg , anti-HBs, anti-T4 and HCVAg were adsorbed with estimated average height * of 0.70-1 μm; 0.4-0.6 μm, 0.75-0.90 μm and 0.7-0.8 μm respectively on the NR surface ( Fig. 2.28). The average size of each cluster was $5.5x10^{-7}$ $cm^2$ for anti-HBs, $1.5x10^{-6}$ $cm^2$ for HBsAg and $3.15x10^{-7}$ $cm^2$ for anti-T4. The coatings of anti-HBs, HBsAg and anti-T4 on polypropylene surface showed a decrease in the amount adsorbed but they were more homogeneous in appearance on the surface probably due to unfolding of protein. The individual molecular heights*, as indicated by the profiles in Fig 2.28 (20-50 nm for HBsAg, 50-60 nm for anti-HBs 30-40 nm for anti-T4 and 50-160 nm for HCVAg respectively ) show a much thinner coating compared to NR surface. Thus they provide larger surface area of interaction between serum antigen or antibody with the immobilised macromolecule. For the NR system, the antigen and antibody clusters formed were partially embedded into the natural rubber layer. Thus the effective sites of antibody or antigen were reduced. Serum antibodies and antigen can only interact with the immobilised protein on the surface of the cluster. Formation of cluster give rise to steric hindrance of binding site of paratope of antibody and epitope of antigen resulting in less effective binding sites of the immobilised antibody or antigen being available.

*The average height of the immobilised macromolecules on the surface was calculated based on three profiles of the z-range on different part of the surface

(iii) The EM micrograph and AFM picture revealed that not all the solid phase surface was covered by proteins. Fig. 2.18(a & b) show that a thin layer of NBCS with tread-like structure was adsorbed on PP surface. On NR surface, adsorption of NBCS showed a different features: the macromolecules covered the whole surface giving a thicker layer (0.3-1μm) when compared with that on PP surface (40-50 nm) (Fig. 2.28). PP surface immobilised with anti-HBs or HBsAg, anti-T4 and HCVAg and blocked by NBCS showed even coatings between the immobilised macromolecules (Fig. 2.20-2.23). The addition of NBCS onto the protein immobilised surface would result in NBCS either adsorbed on the immobilised protein or on the bare PP surface. The adsorbed NBCS on PP surface underwent unfolding similar to the immobilised macromolecules. The packing density of protein was determined by the extent of conformational/unfolding changes. On PP hydrophobic surface and at low protein concentration, the protein molecules underwent structural unfolding resulting in a rather flat adsorbed conformation. The degree of flattening determines the number of surface/protein contact points and thereby the tightness of the surface/protein binding. A flattened protein molecule with several contact points will undergo only limited lateral movement or exchange reactions thus changes in lateral movement was limited. This would limit further adsorption at successive additions of proteins to the PP surface as no exchange of molecules took place. There was no bare PP surface available thus resulting in low non-specific binding. However for NR surface, after blocking with NBCS (Fig. 2.24-2.27), the surface appeared to be fully covered by protein molecules where

NBCS filled up the bare surface. However the high non-specific binding indicate that labelled anti-HBs and HBsAg can penetrate the bound NBCS protein and adsorbed onto the NR surface. Labelled anti-HBs which was a smaller molecules compared to labelled HBsAg was easier to penetrate through the blocker layer. The labelled anti-HBs or HBsAg could also bind non-specifically to the aggregates of immobilised anti-HBs or HBsAg and the blocker. Therefore non-specific binding on anti-HBs on NR immobilised surface was much higher than those on PP . The ability of labelled proteins to penetrate the blocked anti-HBs and HBsAg immobilised-NR surface can be deduced from the further reduction in non-specific binding after incubation with negative control serum. Molecular exchange could also occur in which loosely bound NBCS molecules of the aggregates covering a certain area can be displaced by the labelled molecules from the solution. When labelled HBsAg or anti-HBs was added onto anti-HBs or HBsAg coated surface, they were either adsorbed non-specifically onto NR surface by displacing adsorbed NBCS from the aggregates or specifically onto the immobilised protein. Thus competition between the NR surface and NR immobilised with binders for HBsAg or anti-HBs reduce the specific binding and increase the non-specific binding. The amount of non-specific binding of labelled protein depends both on the number of adsorption sites on the surface and also on the packing of molecules on the sites. This in turn depends on the orientation and conformation of the adsorbed molecules, the eventual lateral movement of the molecules and segments of them on the surface, and on the lateral interaction between the adsorbed molecules. The

adsorption is to a large extent governed by dynamic parameters related to the protein-surface interaction.

Fig. 2.8 Scanning electron micrograph showing (a) original uncoated surface of polypropylene. (Magnification $1x10^4$) (b) unwashed natural rubber coated PP tube. (Magnification $5x10^3$)

(a)

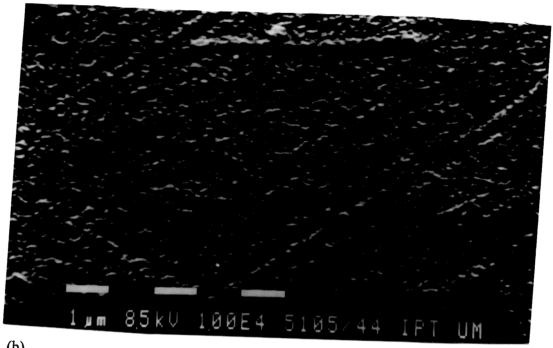


(b)

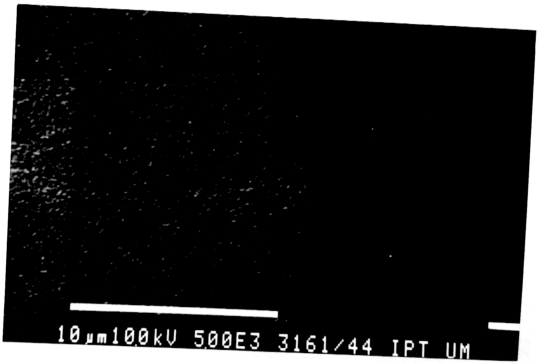

Fig. 2.9 Atomic force microscope images of (a)(i) PP top view surface (10x10 μm) (ii) PP three-dimension surface plot (10x10 μm) (b) (i) Unwashed NR top view surface (10x10 μm) (ii) Unwashed NR three-dimension surface plot (10x10 μm)

a(i)

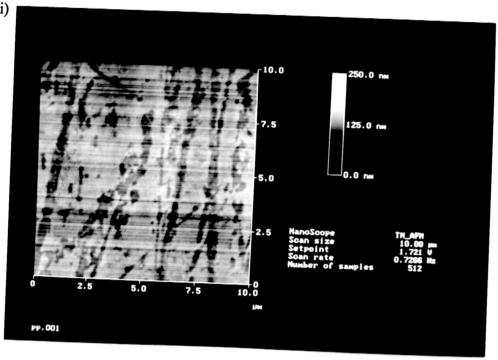


a(ii)

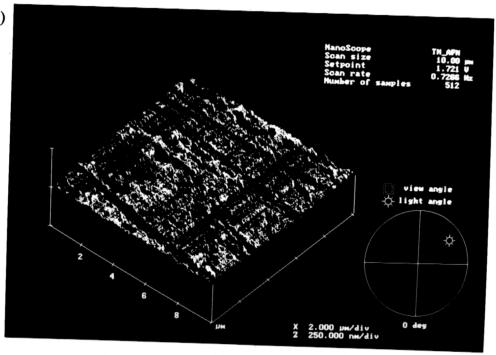

Fig. 2.10(a) Scanning electron micrograph showing PP tube immobilised with HBsAg. Magnification (i) $2x10^3$ (ii)$5x10^3$ (iii) $1x10^4$

200 µl of HBsAg coating solution (1.76 µg/ml) was incubated overnight at 4°C in PP tube, the supernatant was then discarded and the tube was washed four times with 1 ml of distilled water

a(i)

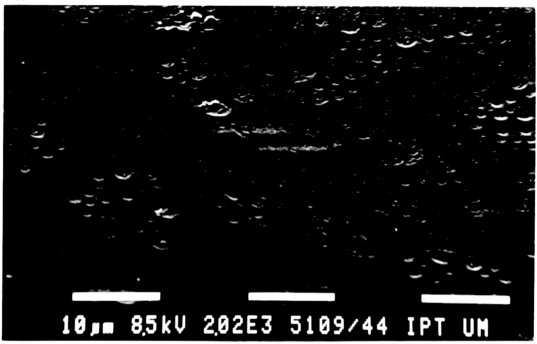


a(ii)

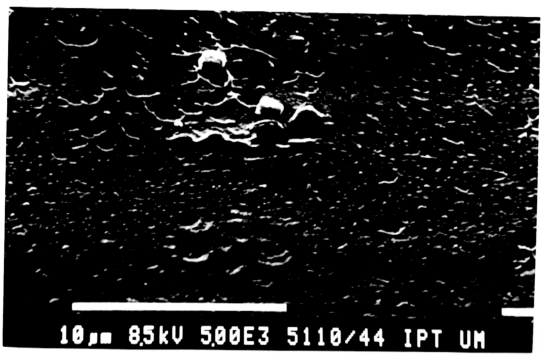

a(iii)

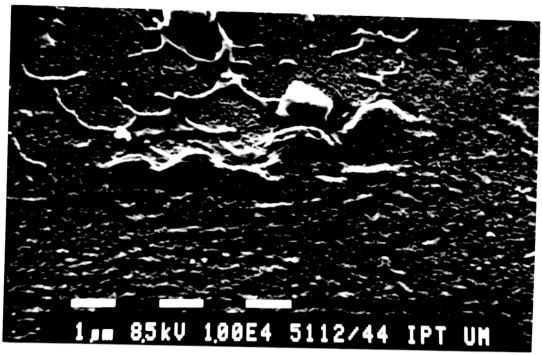

Fig. 2.10 (b) Atomic force microscope images of PP tube immobilised with HBsAg (i) 5x5 µm top view surface (ii) 5x5 µm three dimension surface plot
200 µl of HBsAg coating solution (1.76 µg/ml) was incubated overnight at 4°C in PP tube, the supernatant was then discarded and the tube was washed four times with 1 ml of distilled water

b(i)

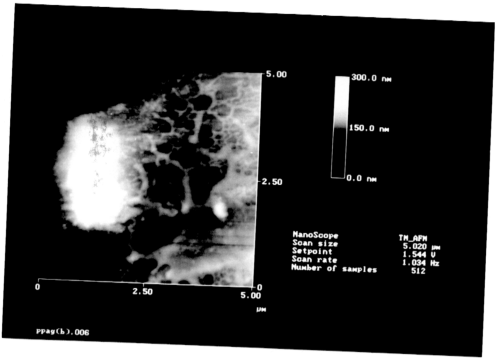


b(ii)

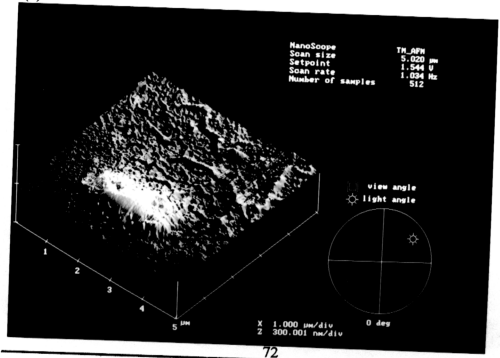

Fig. 2.11(a) Scanning electron micrograph showing PP tube immobilised with Horse anti-HBs. Magnification (i) $2x10^3$ (ii) $1x10^4$

200 µl of anti-HBs coating solution (260 µg/ml) was incubated overnight at 4°C in PP tube, the supernatant was then discarded and the tube was washed four times with 1 ml of distilled water

a(i)

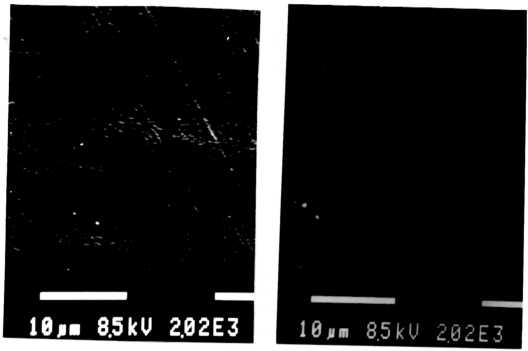


a(ii)

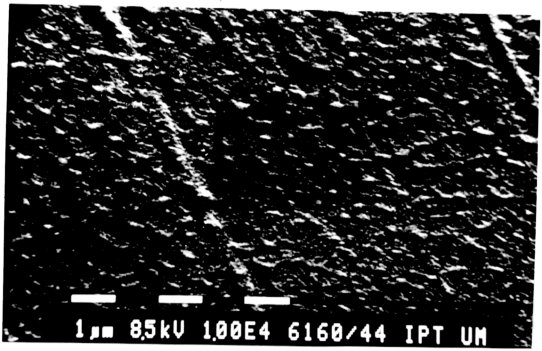

Fig. 2.11 (b) Atomic force microscope images of PP tube immobilised with Horse anti-HBs (i)10 x10 μm top view surface (ii) 10x10 μm three dimension surface plot (iii) 10x10 μm top view surface (iv) 10x 10 μm three dimension surface plot (v) 5x5 μm top view surface (vi) 5x5 μm three dimension surface plot

200 μl of anti-HBs coating solution (260 μg/ml) was incubated overnight at 4°C in PP tube, the supernatant was then discarded and the tube was washed four times with 1 ml of distilled water

b(i)

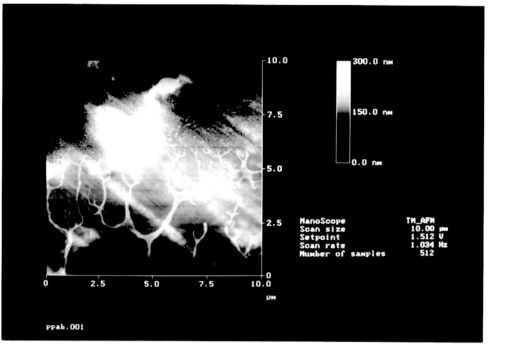


b(ii)

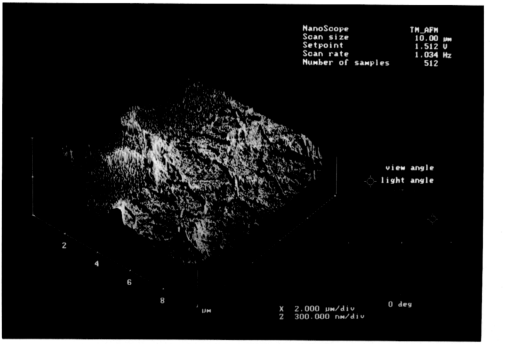

b(iii)

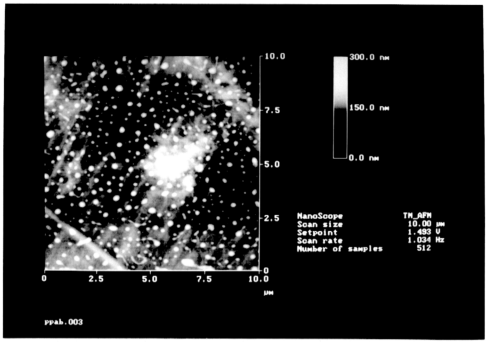
10.0
7.5
5.0
2.5
0
0
2.5
5.0
7.5
10.0
μm
300.0 nm
150.0 nm
0.0 nm
NanoScope
TM_AFM
Scan size
10.00 μm
Setpoint
1.483 V
Scan rate
1.034 Hz
Number of samples
512
ppah.003

b(iv)

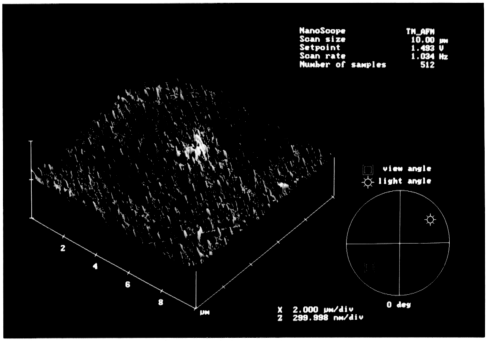
NanoScope
TM_AFM
Scan size
10.00 μm
Setpoint
1.483 V
Scan rate
1.034 Hz
Number of samples
512
view angle
light angle
2
4
6
8
μm
X 2.000 μm/div
Z 299.998 nm/div
0 deg

b(v)

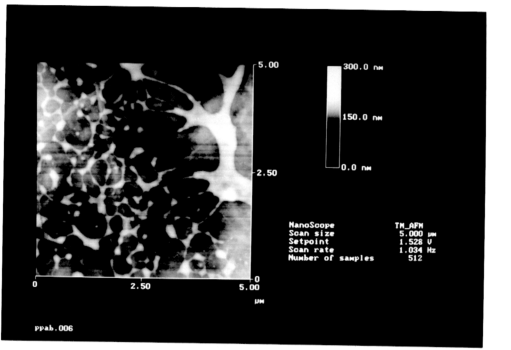
5.00
2.50
0
0
2.50
5.00
μm
300.0 nm
150.0 nm
0.0 nm
NanoScope
Scan size
Setpoint
Scan rate
Number of samples
TM_AFM
5.000 μm
1.528 V
1.034 Hz
512
PPab.006

b(vi)

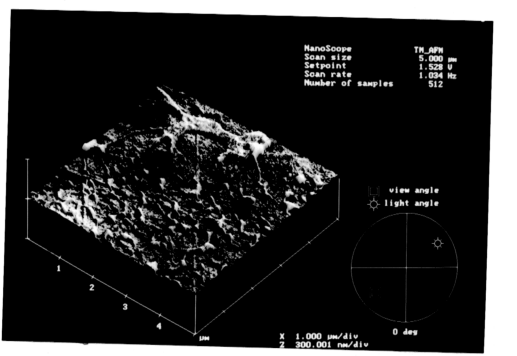
NanoScope
Scan size
Setpoint
Scan rate
Number of samples
TM_AFM
5.000 μm
1.528 V
1.034 Hz
512
view angle
light angle
1
2
3
4
μm
X 1.000 μm/div
Z 300.001 nm/div
0 deg

Fig. 2.12(a) Scanning electron micrograph showing PP tube immobilised with anti-T4. Magnification (i) $2x10^3$ (ii) $1x10^4$

200 µl of anti-T4 (sheep anti-sera) coating solution at a concentration of 1.1 mg/ml was incubated overnight at 4°C in PP tube, the supernatant was then discarded and the tube was washed four times with 1 ml of distilled water.

a(i)


a(ii)

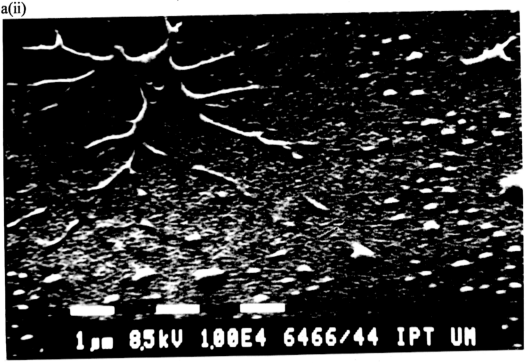

Fig. 2.12 (b) Atomic force microscope images of PP tube immobilised with anti-T4 (i) 5x5 μm top view surface (ii) 5x5 μm three dimension surface plot (iii) 2x2 μm top view surface (v) 2x2 μm three dimension surface plot

200 μl of anti-T4 (sheep anti-sera) coating solution at a concentration of 1.1 mg/ml was incubated overnight at 4°C in PP tube, the supernatant was then discarded and the tube was washed four times with 1 ml of distilled water.

b(i)

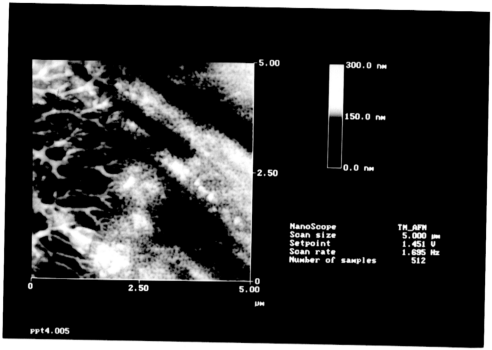


b(ii)

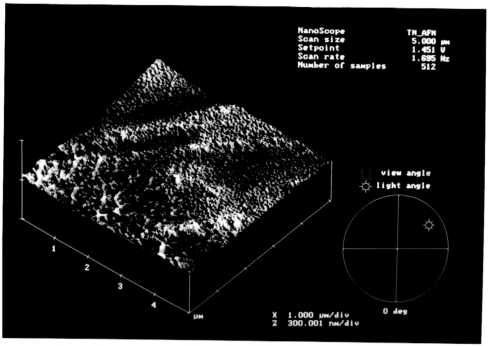

b(iii)

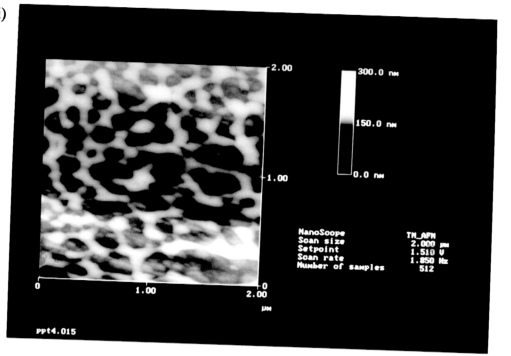
2.00
1.00
0
1.00
2.00
μm
300.0 nm
150.0 nm
0.0 nm
NanoScope
Scan size
Setpoint
Scan rate
Number of samples
TM_AFM
2.000 μm
1.510 V
1.850 Hz
512
PPt4.015

b(iv)

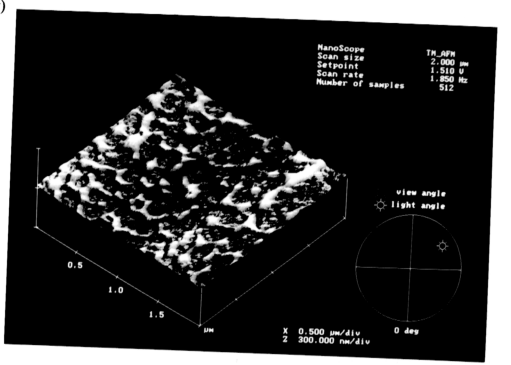
NanoScope
Scan size
Setpoint
Scan rate
Number of samples
TM_AFM
2.000 μm
1.510 V
1.850 Hz
512
view angle
light angle
0.5
1.0
1.5
μm
X 0.500 μm/div
Z 300.000 nm/div
0 deg

Fig. 2.13 Atomic force microscope images of PP tube immobilised with HCVAg (i)10 x10 μm top view surface (ii) 10x10 μm three dimension surface plot (iii) 5x5 μm top view surface (iv) 5x5 μm three dimension surface plot

200 μl of HCVAg coating solution ( 1μg/ml) was incubated overnight at 4°C in PP tube, the supernatant was then discarded and the tube was washed four times with 1 ml of distilled water

(i)

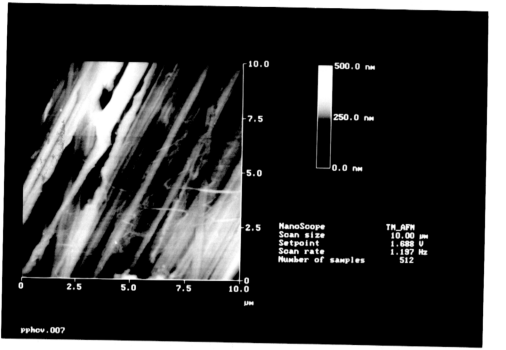


(ii)

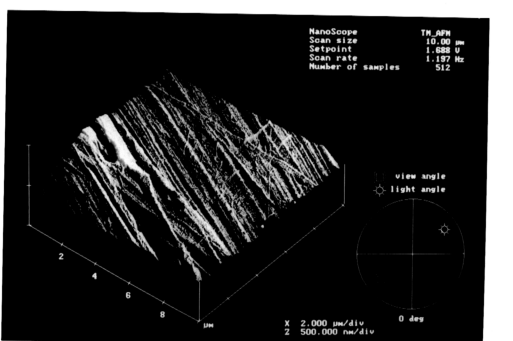

(iii)

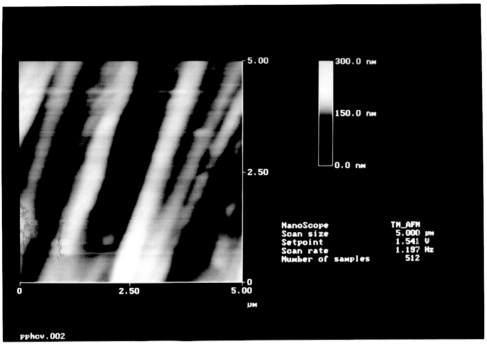
5.00
2.50
0
0
2.50
5.00
μm
300.0 nm
150.0 nm
0.0 nm
NanoScope TM_AFN
Scan size 5.000 μm
Setpoint 1.541 V
Scan rate 1.197 Hz
Number of samples 512
pyhcv.002

(iv)

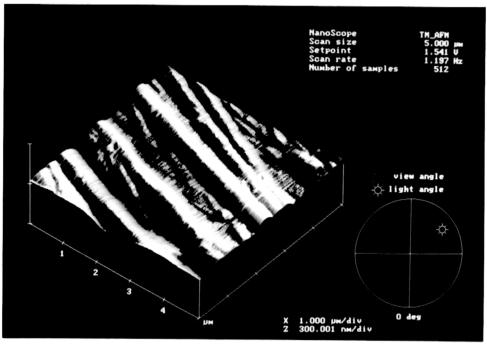
NanoScope TM_AFN
Scan size 5.000 μm
Setpoint 1.541 V
Scan rate 1.197 Hz
Number of samples 512
view angle
light angle
1
2
3
4
μm
X 1.000 μm/div
Z 300.001 nm/div
0 deg

Fig. 2.14 (a) Scanning electron micrograph showing WNR tube with HBsAg. Magnification (i) $2x10^3$ (ii) $1x10^4$

200 µl of HBsAg coating solution (1.76µg/ml) was incubated overnight at 4°C in WNR tube, (NR coated tube prewashed five times with 1 ml of 0.1M HCl followed by five washes with 1 ml of distilled water) , the supernatant was then discarded and the tube was washed four times with 1 ml of distilled water.

a(i)


a(ii)

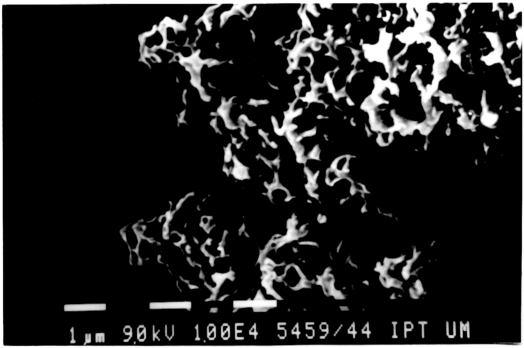

Fig. 2.14(b) Atomic force microscope images of WNR tube immobilised with HBsAg (i) 10x10 μm top view surface (ii) 10x10 μm three dimension surface

200 μl of HBsAg coating solution (1.76 μg/ml) was incubated overnight at 4°C in WNR tube, (NR coated tube prewashed five times with 1 ml of 0.1M HCl followed by five washes with 1 ml of distilled water) , the supernatant was then discarded and the tube was washed four times with 1 ml of distilled water.

b(i)

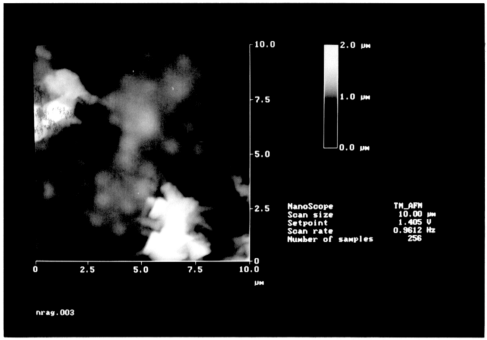


b(ii)

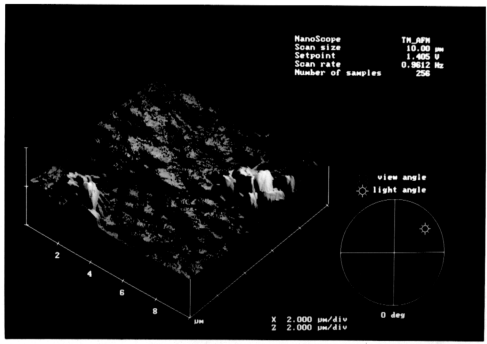

Fig. 2.15 (a) Scanning electron micrograph showing WNR tube immobilised with anti-HBs. Magnification (i) $2x10^3$ (ii) $1x10^4$

200 µl of anti-HBs coating solution (260 µg/ml) was incubated overnight at 4°C in WNR tube, (NR coated tube prewashed five times with 1 ml of 0.1M HCl followed by five washes with 1 ml of distilled water) , the supernatant was then discarded and the tube was washed four times with 1 ml of distilled water

a(i)

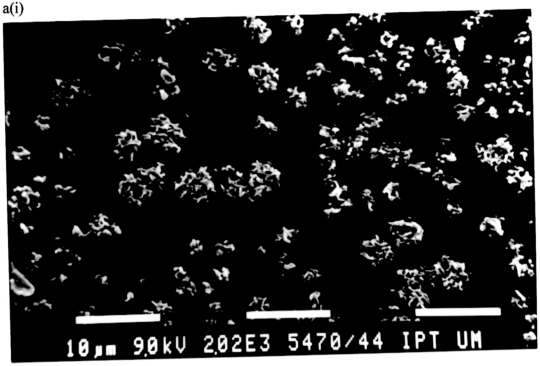


b(ii)

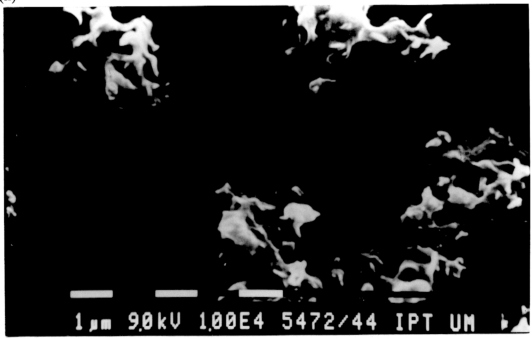

Fig. 2.15 (b) Atomic force microscope images of WNR tube immobilised with anti-HBs (i) 10x10 μm top view surface (ii)10x10 μm three dimension surface

200 μl of anti-HBs coating solution (260 μg/ml) was incubated overnight at 4°C in WNR tube, (NR coated tube prewashed five times with 1 ml of 0.1M HCl followed by five washes with 1 ml of distilled water) , the supernatant was then discarded and the tube was washed four times with 1 ml of distilled water.

b(i)

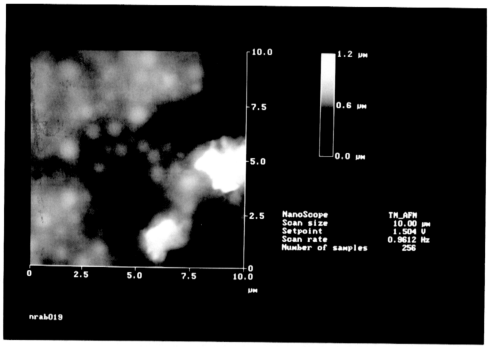


b(ii)

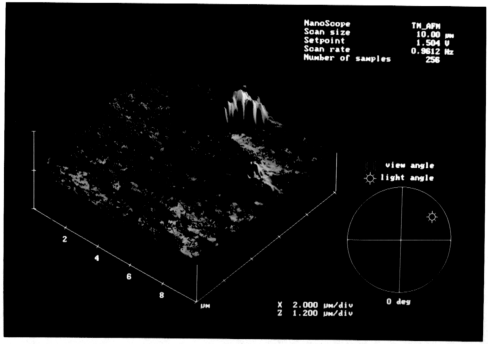

Fig. 2.16 (a) Scanning electron micrograph showing WNR tube immobilised with anti-T4. Magnification (i) $2x10^3$ (ii) $1x10^4$

200 µl of anti-T4 (sheep anti-sera) coating solution at a concentration of 1.1 mg/ml was incubated overnight at 4°C in WNR tube (NR coated tube prewashed five times with 1 ml of 0.1M HCl followed by five washes with 1 ml of distilled water) , the supernatant was then discarded and the tube was washed four times with 1 ml of distilled water.

a(i)

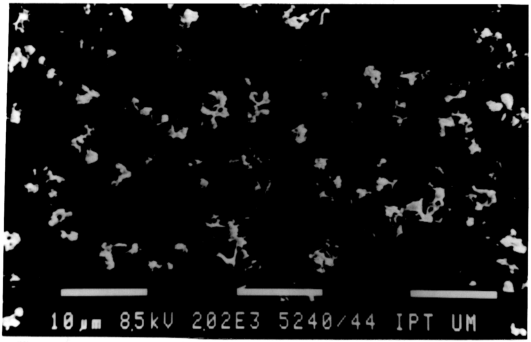


a(ii)

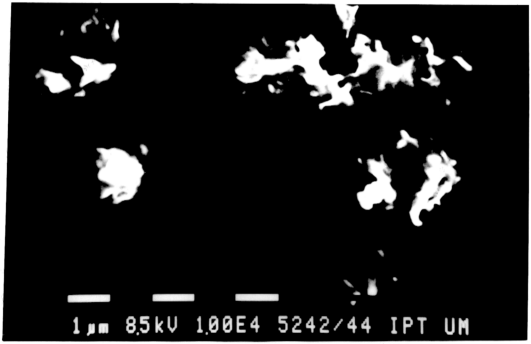

Fig. 2.16 (b) Atomic force microscope images of WNR tube immobilised with anti-T4 (i) 10x10 μm top view surface (ii) 10x10 μm three dimension surface

200 μl of anti-T4 coating solution at a concentration of 1.1 mg/ml was incubated overnight at 4°C in WNR tube (NR coated tube prewashed five times with 1 ml of 0.1M HCl followed by five washes with 1 ml of distilled water), the supernatant was then discarded and the tube was washed four times with 1 ml of distilled water.

b(i)

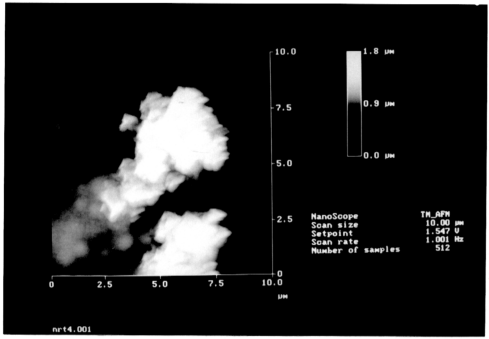


b(ii)

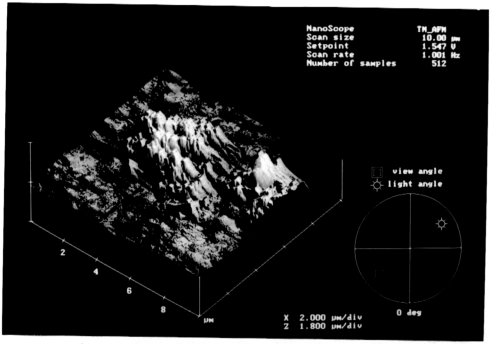

Fig. 2.17 Atomic force microscope images of WNR tube immobilised with HCVAg (i) 10x10μm top view surface (ii) 10x10μm three dimension surface

200 μl of HCVAg coating solution ( 1μg/ml) was incubated overnight at 4°C in WNR tube (NR coated tube prewashed five times with 1 ml of 0.1M HCl followed by five washes with 1 ml of distilled water) , the supernatant was then discarded and the tube was washed four times with 1 ml of distilled water.

(i)

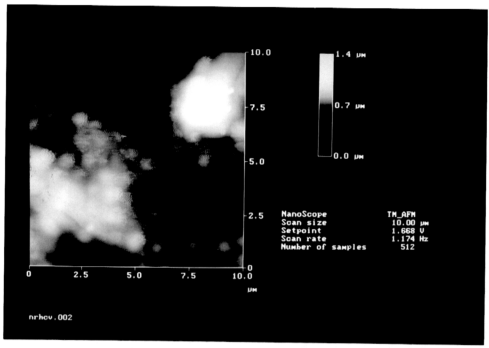


(ii)

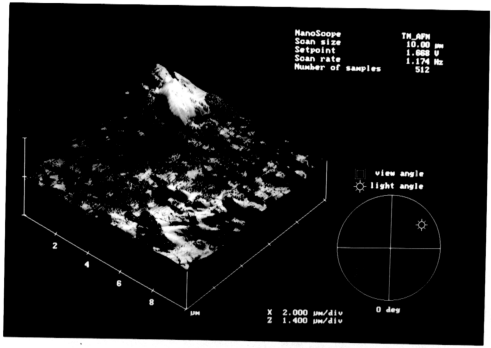

Fig. 2.18 (a) Scanning electron micrograph showing PP tube immobilised with 50% NBCS. Magnification (i) $2x10^3$ (ii) $1x10^4$
200 µl of 50% NBCS was incubated overnight at 4°C in PP tube, the supernatant was then discarded and washed four times with 1 ml of distilled water

a(i)

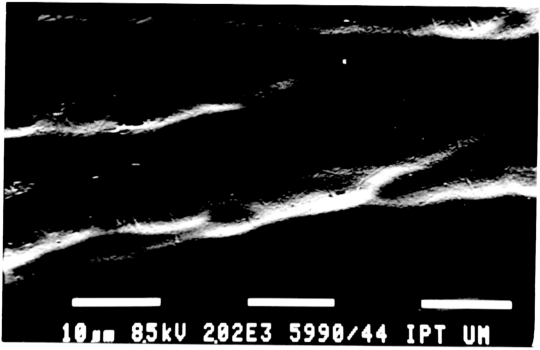


a(ii)

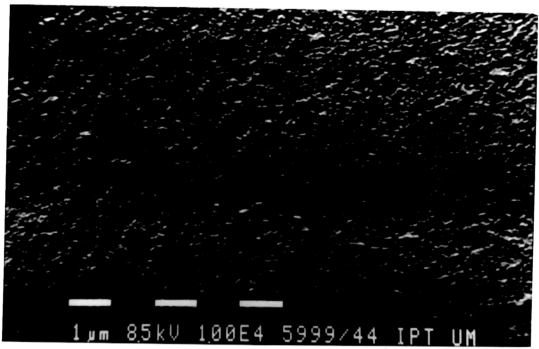

Fig. 2.18(b) Atomic force microscope images of PP tube immobilised with 50% NBCS (i) 5x5 µm top view surface (ii) 5x5 µm three dimension surface (iii) 2x2 µm top view surface (iv) 2x2 µm three dimension surface (v) 2x2 µm top view surface (vi) 2x2 µm three dimension surface

200 µl of 50% NBCS was incubated overnight at 4°C in PP tube, the supernatant was then discarded and the tube was washed four times with 1 ml of distilled water

b(i)

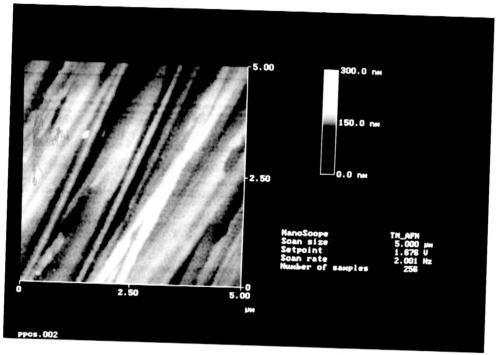


b(ii)

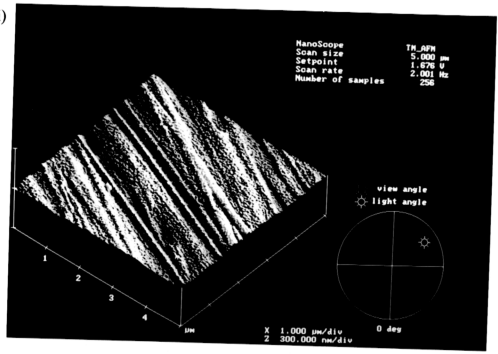

b(iii)

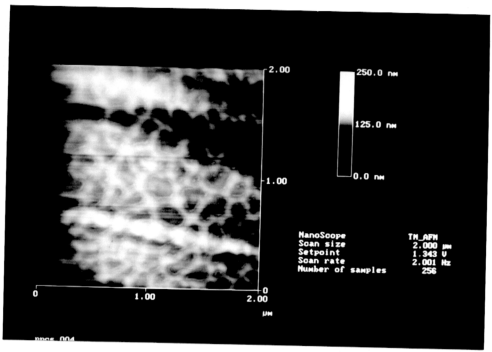
2.00
1.00
0
1.00
2.00
μm
250.0 nm
125.0 nm
0.0 nm
NanoScope
Scan size
Setpoint
Scan rate
Number of samples
TM_AFM
2.000 μm
1.343 V
2.001 Hz
256

b(iv)

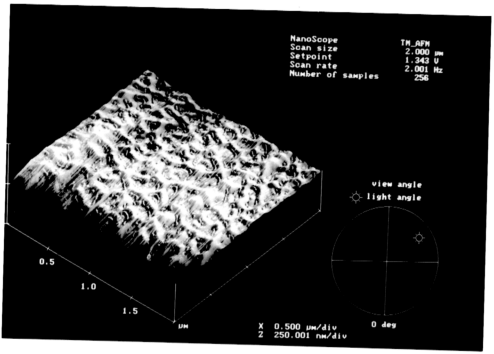
NanoScope
Scan size
Setpoint
Scan rate
Number of samples
TM_AFM
2.000 μm
1.343 V
2.001 Hz
256
view angle
light angle
0.5
1.0
1.5
μm
X 0.500 μm/div
Z 250.001 nm/div
0 deg

b(v)

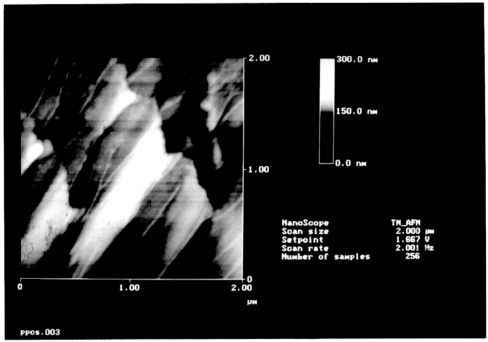
2.00
1.00
0
0
1.00
2.00
μm
300.0 nm
150.0 nm
0.0 nm
NanoScope
Scan size
Setpoint
Scan rate
Number of samples
TM_AFM
2.000 μm
1.667 V
2.001 Hz
256
ppcs.003

b(vi)

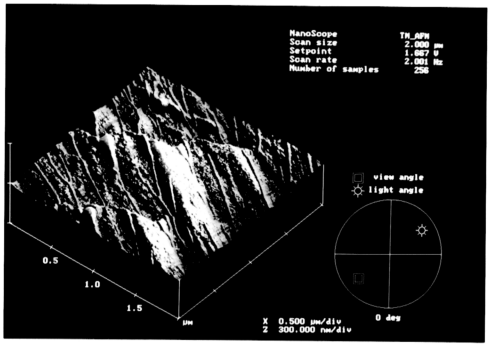
NanoScope
Scan size
Setpoint
Scan rate
Number of samples
TM_AFM
2.000 μm
1.667 V
2.001 Hz
256
view angle
light angle
0.5
1.0
1.5
μm
X 0.500 μm/div
Z 300.000 nm/div
0 deg

Fig. 2.19 (a) Scanning electron micrograph showing WNR tube immobilised with 50% NBCS. Magnification (i)$2x10^3$ (ii) $1x10^4$

200 µl of 50% NBCS was incubated overnight at 4°C in WNR tube (NR coated tube prewashed five times with 1 ml of 0.1M HCl followed by five washes with 1 ml of distilled water), the supernatant was then discarded and the tube was washed four times with 1 ml of distilled water.

a(i)

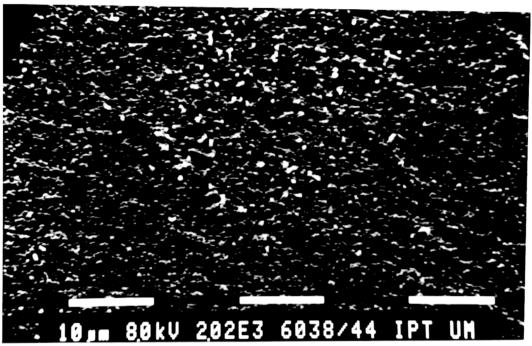


a(ii)

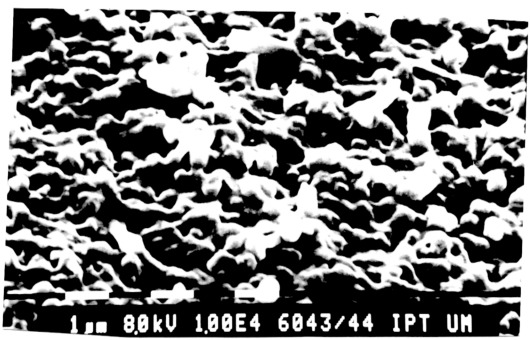

Fig. 2.19(b) Atomic force microscope images of WNR tube immobilised with 50% NBCS (i) 10x10 μm top view surface (ii) 10x10 μm three dimension surface
200μl of 50% NBCS was incubated overnight at 4°C in WNR tube (NR coated tube prewashed five times with 1 ml of 0.1M HCl followed by five washes with 1 ml of distilled water) , the supernatant was then discarded and the tube was washed four times with 1 ml of distilled water.

b(i)

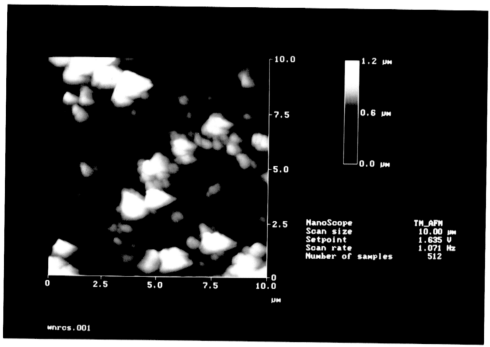


b(ii)

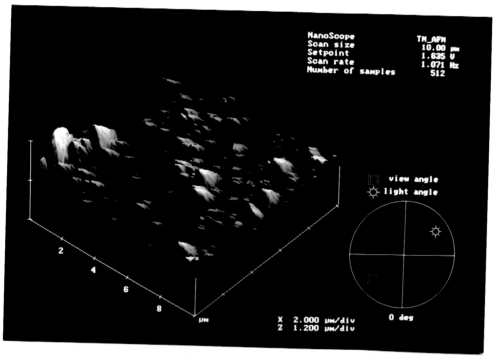

Fig. 2.20(a) Scanning electron micrograph showing PP tube immobilised with HBsAg and 50% NBCS. Magnification (i)$1x10^3$ (ii) $2x10^3$ (iii)$5x10^3$ (iv)$5x10^3$
200 µl of HBsAg coating solution (1.76µg/ml) was incubated overnight at 4°C in PP tube , the supernatant was then discarded and the tube was washed four times with 1 ml of distilled water. The tube was then blocked with 50% NBCS at 4°C for overnight and followed by four washes with 1 ml of distilled water.

a(i)


a(ii)

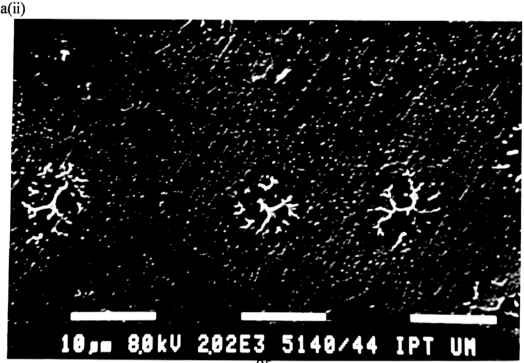

a(iii)

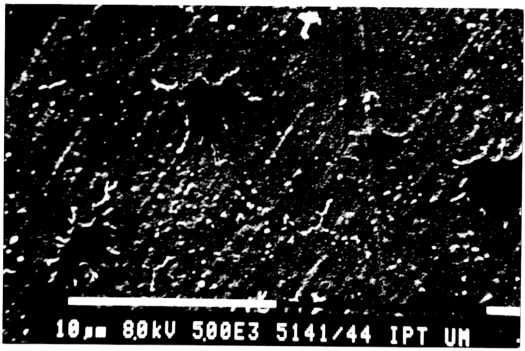


a(iv)

Fig. 2.20 (b) Atomic force microscope images of PP tube immobilised with HBsAg and 50% NBCS (i) 10x10 μm top view surface (ii) 10x10 μm three dimension surface (iii) 5x5 μm top view surface (iv) 5x5 μm three dimension surface ( v) 2x2 μm top view surface (vi) 2x2 μm three dimension surface

200 μl of HBsAg coating solution (1.76μg/ml) was incubated overnight at 4°C in PP tube , the supernatant was then discarded and the tube was washed four times with 1 ml of distilled water. The tube was then blocked with 50% NBCS at 4°C for overnight and followed by four washes with 1 ml distilled water.

b(i)

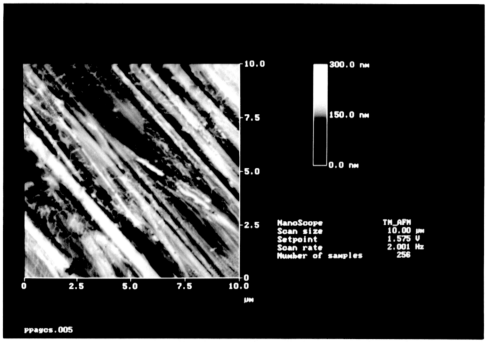


b(ii)

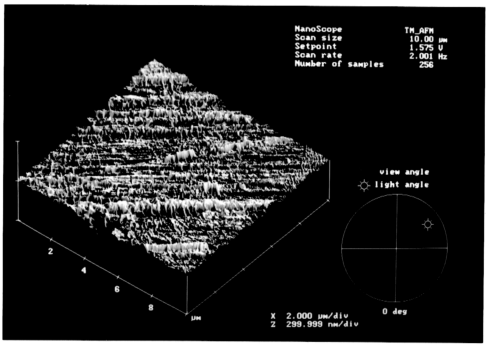

b(iii)


5.00
2.50
0
2.50
5.00
μm
300.0 nm
150.0 nm
0.0 nm
NanoScope
Scan size
Setpoint
Scan rate
Number of samples
TM_APM
5.039 μm
1.693 V
2.001 Hz
256
PPapcsCb.001

b(iv)

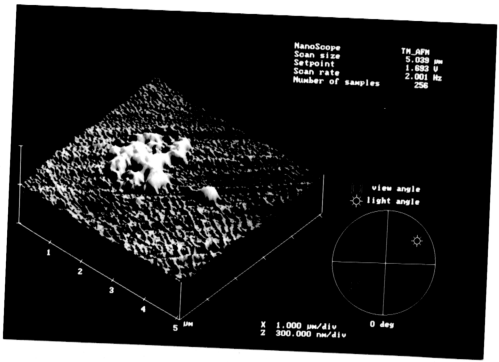
NanoScope
Scan size
Setpoint
Scan rate
Number of samples
TM_APM
5.039 μm
1.693 V
2.001 Hz
256
view angle
light angle
1
2
3
4
5 μm
X 1.000 μm/div
Z 300.000 nm/div
0 deg

(v)

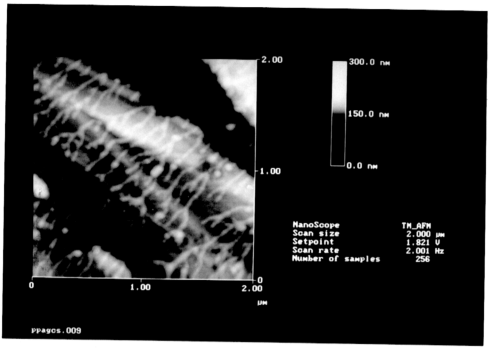
2.00
1.00
0
1.00
2.00
μm
300.0 nm
150.0 nm
0.0 nm
NanoScope
Scan size
Setpoint
Scan rate
Number of samples
TM_AFM
2.000 μm
1.821 V
2.001 Hz
256
ppaycs.009

(vi)

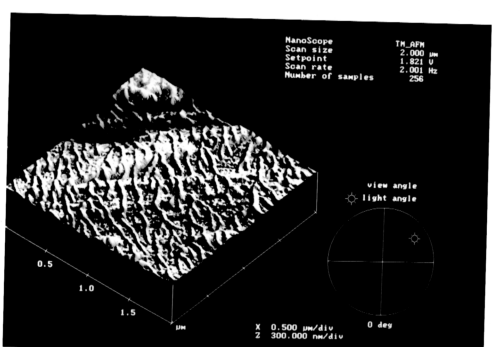
NanoScope
Scan size
Setpoint
Scan rate
Number of samples
TM_AFM
2.000 μm
1.821 V
2.001 Hz
256
view angle
light angle
0.5
1.0
1.5
μm
X 0.500 μm/div
Z 300.000 nm/div
0 deg

Fig.2.21 (a) Scanning electron micrograph showing PP tube immobilised with anti-HBs and 50% NBCS. Magnification (i) $2x10^3$ (ii) $1x10^4$

200 µl of anti-HBs coating solution (260µg/ml) was incubated overnight at 4°C in PP tube , the supernatant was then discarded and the tube was washed four times with 1 ml distilled water. The tube was then blocked with 50% NBCS at 4°C for overnight and followed by four washes with 1 ml of distilled water .

a(i)

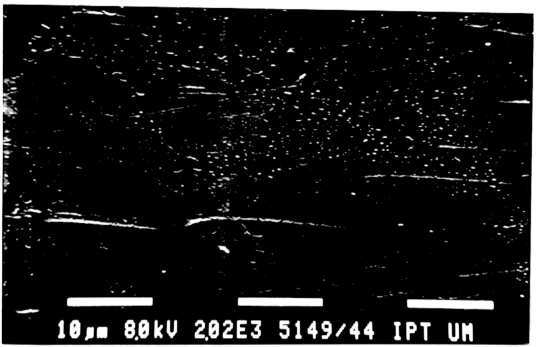


a(ii)

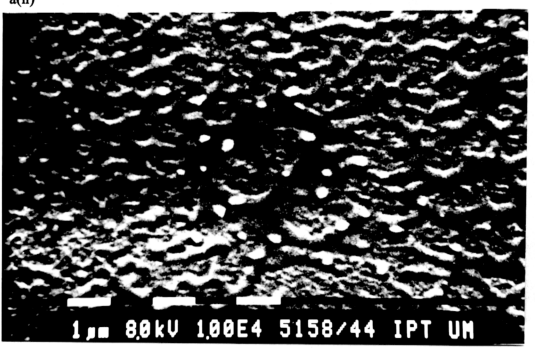

Fig. 2.21 (b) Atomic force microscope images of PP tube immobilised with anti-HBs and 50% NBCS (i) 10x10 μm top view surface (ii) 10x10 μm three dimension surface (iii) 5x5 μm top view surface (iv)5x5 μm three dimension surface plot
200 μl of anti-HBs coating solution (260 μg/ml) was incubated overnight at 4°C in PP tube, the supernatant was then discarded and the tube was washed four times with 1 ml of distilled water. The tube was then blocked with 50% NBCS at 4°C for overnight and followed by four washes with 1 ml of distilled water.

b(i)

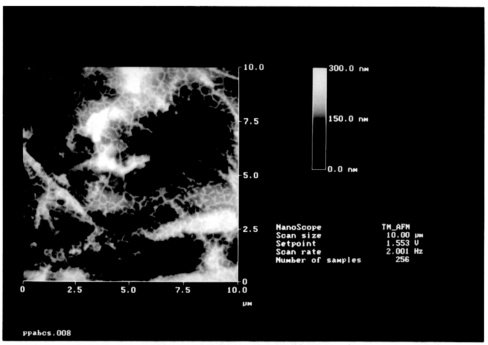


b(ii)

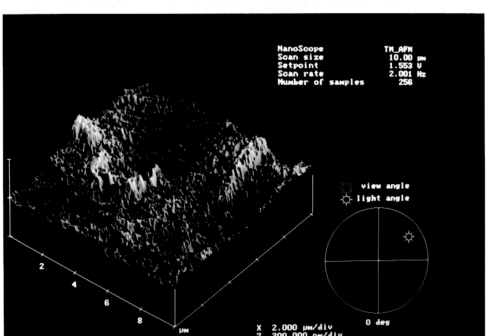

b(iii)

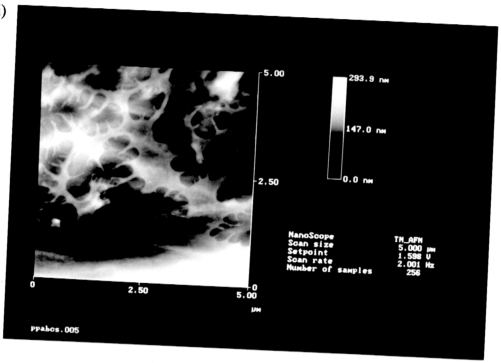
5.00
2.50
0
2.50
5.00
μm
293.8 nm
147.0 nm
0.0 nm
NanoScope
Scan size
Setpoint
Scan rate
Number of samples
TM_AFM
5.000 μm
1.500 V
2.001 Hz
256
PPahos.005

b(iv)

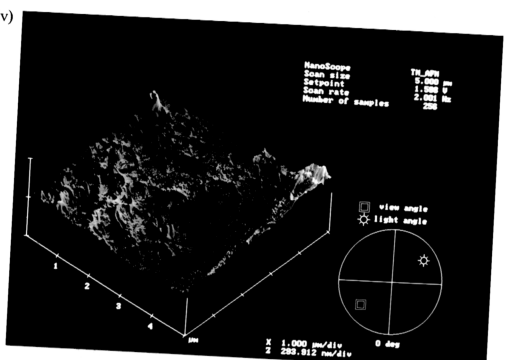
NanoScope
Scan size
Setpoint
Scan rate
Number of samples
TM_AFM
5.000 μm
1.500 V
2.001 Hz
256
view angle
light angle
1
2
3
4
μm
X 1.000 μm/div
Z 293.912 nm/div
0 deg

Fig. 2.22 Atomic force microscope images of PP tube immobilised with anti-T4 and 50% NBCS (i)5x5 μm top view surface (ii)5x5 μm three dimension surface (iii)2.5x2.5 μm top view surface (iv)2.5x2.5 μm three dimension surface plot (v)2x2 μm top view surface (vi)2x2 μm three dimension surface plot

200 μl of anti-T4 ( sheep anti-sera) coating solution at a concentration of 1.1 mg/ml was incubated overnight at 4°C in PP tube , the supernatant was then discarded and the tube was washed four times with 1 ml of distilled water. The tube was then blocked with 50% NBCS at 4°C for overnight and followed by four washes of 1 ml distilled water

(i)

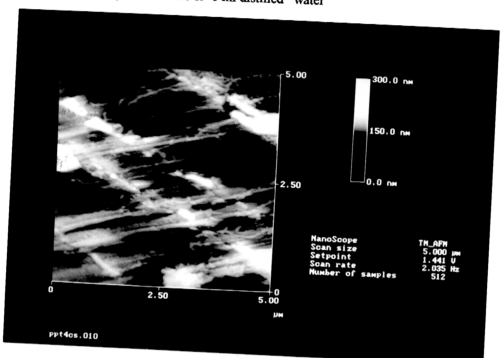


(ii)

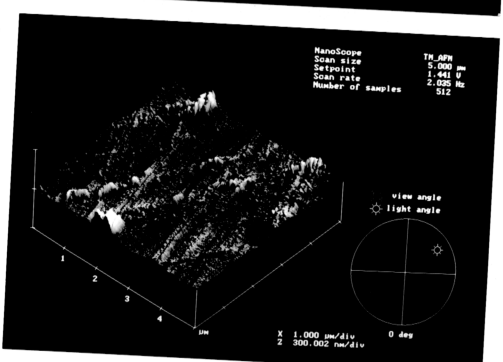

(iii)

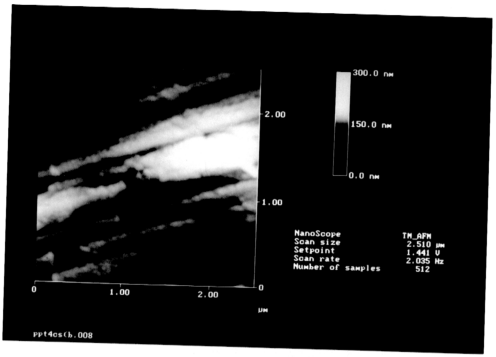
300.0 nm
150.0 nm
0.0 nm
2.00
1.00
0
1.00
2.00
μm
NanoScope
Scan size
Setpoint
Scan rate
Number of samples
TM_AFM
2.510 μm
1.441 V
2.035 Hz
512
ppt4csCb.008

(iv)

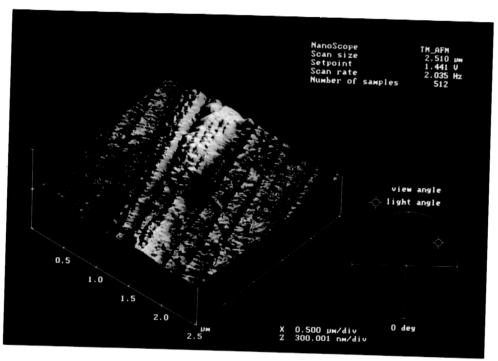
NanoScope
Scan size
Setpoint
Scan rate
Number of samples
TM_AFM
2.510 μm
1.441 V
2.035 Hz
512
view angle
light angle
0.5
1.0
1.5
2.0
2.5
μm
X 0.500 μm/div
Z 300.001 nm/div
0 deg

(v)

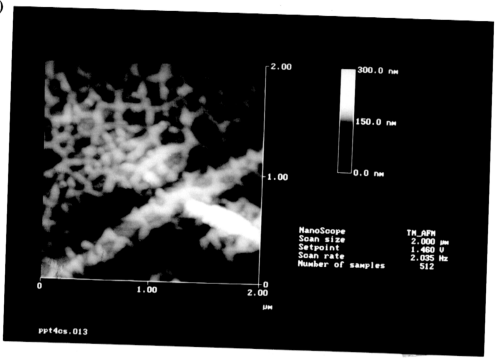
2.00
1.00
0
1.00
2.00
μm
300.0 nm
150.0 nm
0.0 nm
NanoScope
Scan size
Setpoint
Scan rate
Number of samples
TM_AFM
2.000 μm
1.460 V
2.035 Hz
512
ppt4cs.013

(vi)

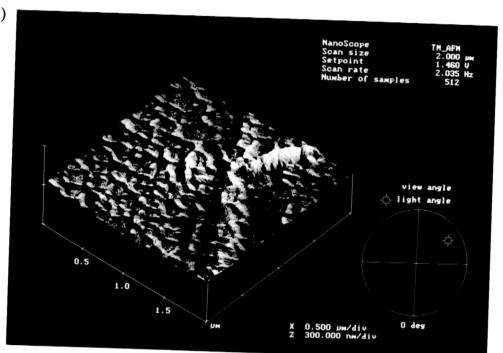
NanoScope
Scan size
Setpoint
Scan rate
Number of samples
TM_AFM
2.000 μm
1.460 V
2.035 Hz
512
view angle
light angle
0.5
1.0
1.5
μm
X 0.500 μm/div
Z 300.000 nm/div
0 deg

Fig. 2.23 Atomic force microscope images of PP tube immobilised with HCVAg and 50% NBCS (i) 10x10 μm top view surface (ii) 10x10 μm three dimension surface (iii) 5x5 μm top view surface (iv) 5x5 μm three dimension surface plot

200 μl of HCVAg coating solution (1 μg/ml) was incubated overnight at 4°C in PP tube , the supernatant was then discarded and the tube was washed four times with 1 ml distilled water. The tube was then blocked with 50% NBCS at 4°C for overnight and followed by four washes of 1 ml distilled water

(i)

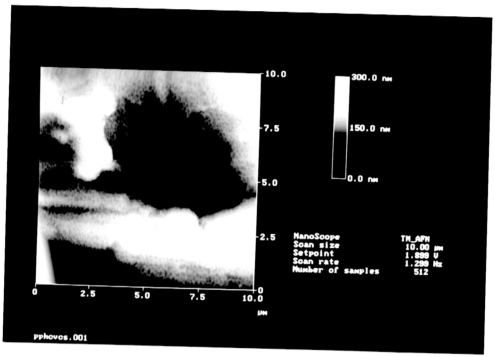


(ii)

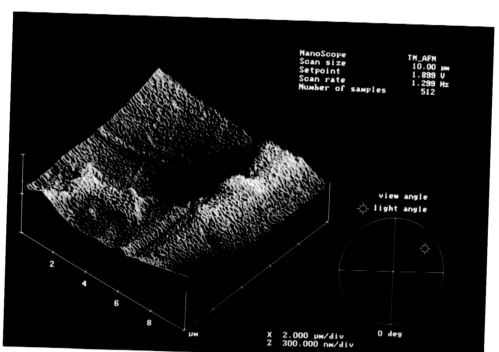

(iii)

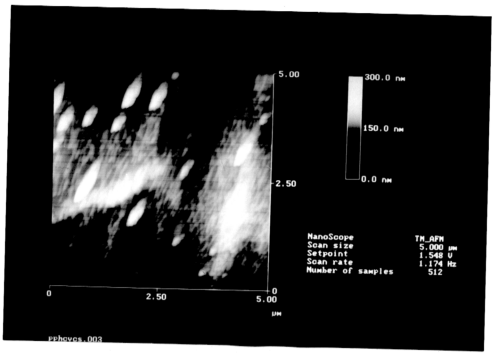
5.00
2.50
0
0
2.50
5.00
μm
300.0 nm
150.0 nm
0.0 nm
NanoScope
Scan size
Setpoint
Scan rate
Number of samples
TM_AFM
5.000 μm
1.548 V
1.174 Hz
512
rphcvgs 003

(iv)

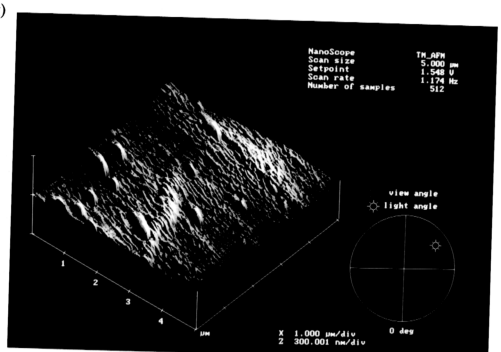
NanoScope
Scan size
Setpoint
Scan rate
Number of samples
TM_AFM
5.000 μm
1.548 V
1.174 Hz
512
view angle
light angle
1
2
3
4
μm
X 1.000 μm/div
Z 300.001 nm/div
0 deg

Fig. 2.24(a) Scanning electron micrograph showing WNR tube immobilised with HBsAg and 50% NBCS. Magnification (i) $2x10^3$ (ii) $1x10^4$

200 µl of HBsAg coating solution (1.76µg/ml) was incubated overnight at 4°C in WNR tube, (NR coated tube prewashed five times with 1 ml of 0.1M HCl followed by five washes with 1 ml of distilled water) , the supernatant was then discarded and the tube was washed four times with 1 ml of distilled water. The tube was then blocked with 50% NBCS at 4°C for overnight and followed by four washes with 1 ml of distilled water.

a(i)

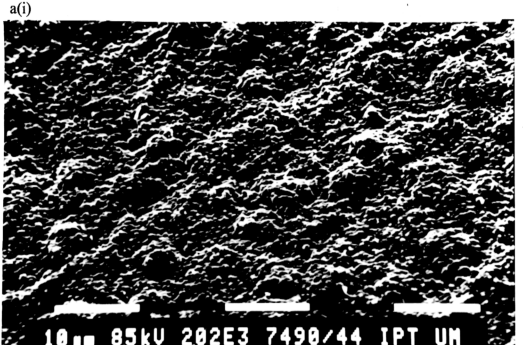


a(ii)

Fig. 2.24 (b) Atomic force microscope images of WNR tube immobilised with HBsAg and 50% NBCS (i) 10x10μm top view surface (ii) 10x10 μm three dimension surface

200 μl of HBsAg coating solution (1.76 μg/ml) was incubated overnight at 4°C in WNR tube(NR coated tube prewashed five times with 1 ml of 0.1M HCl followed by five washes with 1 ml of distilled water) , the supernatant was then discarded and the tube was washed four times with 1 ml of distilled water. The tube was then blocked with 50% NBCS at 4°C for overnight and followed by four washes with 1 ml of distilled water .

b(i)

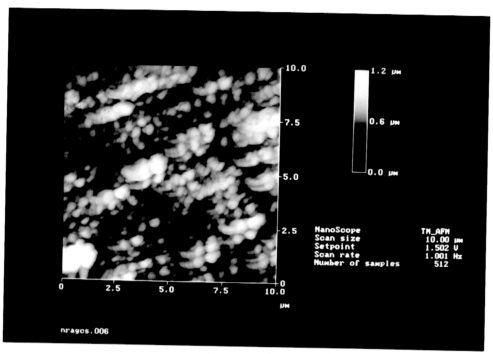


b(ii)

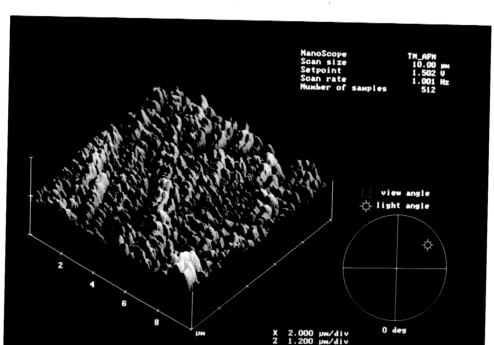

Fig. 2.25 (a) Scanning electron micrograph showing WNR tube with anti-HBs and 50% NBCS. Magnification (i) $2x10^3$ (ii) $1x10^4$

200 µl of anti-HBs coating solution (260 µg/ml) was incubated overnight at 4°C in WNR tube (NR coated tube prewashed five times with 1 ml of 0.1M HCl followed by five washes with 1 ml of distilled water) , the supernatant was then discarded and the tube was washed four times with 1 ml of distilled water. The tube was then blocked with 50% NBCS at 4°C for overnight and followed by four washes with 1 ml of distilled water.

a(i)

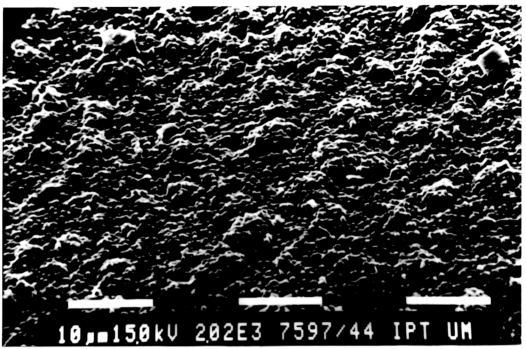


a(ii)

Fig. 2.25 (b) Atomic force microscope images of WNR tube immobilised with anti-HBs and 50% NBCS (i) 10x10μm top view surface (ii) 10x10 μm three dimension surface

200μl of anti-HBs coating solution (260 μg/ml) was incubated overnight at 4°C in WNR tube (NR coated tube prewashed five times with 1 ml of 0.1M HCl followed by five washes with 1 ml of distilled water) , the supernatant was then discarded and the tube was washed four times with 1 ml of distilled water. The tube was then blocked with 50% NBCS at 4°C for overnight and followed by four washes with 1 ml of distilled water .

b(i)

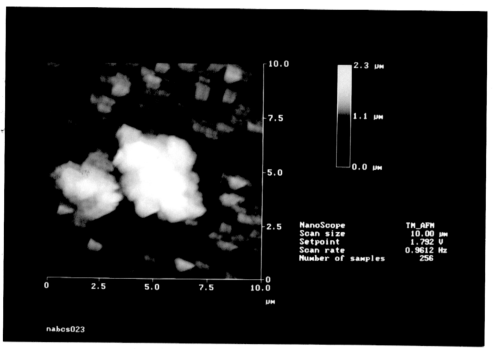


b(ii)

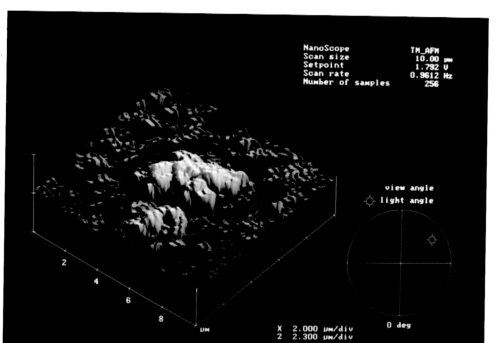

Fig. 2.26 (a) Scanning electron micrograph showing WNR tube immobilised with anti-T4 and 50% NBCS. Magnification (i) $2x10^3$ (ii) $1x10^4$

200 µl of anti-T4 coating solution at a concentration of 1.1 mg/ml was incubated overnight at 4°C in WNR tube, (NR coated tube prewashed five times with 1 ml of 0.1M HCl followed by five washes with 1 ml of distilled water) , the supernatant was then discarded and the tube was washed four times with 1 ml of distilled water. The tube was then blocked with 50% NBCS at 4°C for overnight and followed by four washes with 1 ml of distilled water .

a(i)

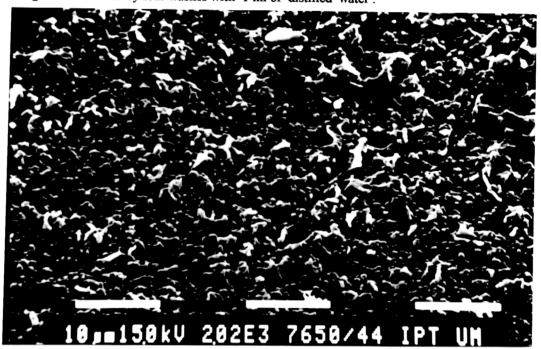


a(ii)

Fig. 2.26 (b) Atomic force microscope images of WNR tube immobilised with anti-T4 and 50% NBCS (i) 10x10μm top view surface (ii) 10x10 μm three dimension surface

200μl of anti-T4 coating solution (1.1 mg/ml) was incubated overnight at 4°C in WNR tube (NR coated tube prewashed five times with 1 ml of 0.1M HCl followed by five washes with 1 ml of distilled water) , the supernatant was then discarded and the tube was washed four times with 1 ml of distilled water. The tube was then blocked with 50% NBCS at 4°C for overnight and followed by four washes with 1 ml of distilled water.

b(i)


b(ii)

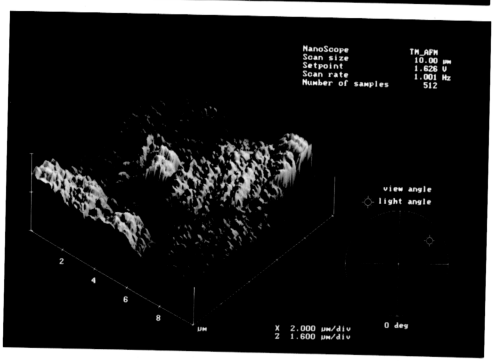

Fig. 2.27 Atomic force microscope images of WNR tube immobilised with HCVAg and 50% NBCS (i) 10x10μm top view surface (ii) 10x10μm three dimension surface (iii) 10x10μm top view surface (iv) 10x10μm three dimension surface

200 μl of HCVAg coating solution (1 μg/ml) was incubated overnight at 4°C in WNR tube, (NR coated tube prewashed five times with 1 ml of 0.1M HCl followed by five washes with 1 ml of distilled water) , the supernatant was then discarded and the tube was washed four times with 1 ml of distilled water. The tube was then blocked with 50% NBCS at 4°C for overnight and followed by four washes with 1 ml of distilled water.

(i)

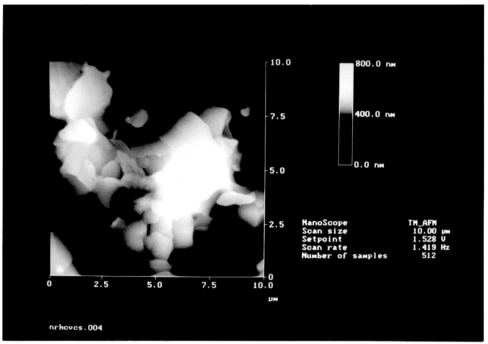


(ii)

(iii)

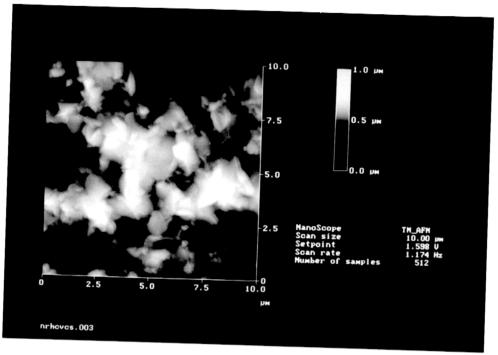
10.0
7.5
5.0
2.5
0
0
2.5
5.0
7.5
10.0
μm
1.0 μm
0.5 μm
0.0 μm
NanoScope
Scan size
Setpoint
Scan rate
Number of samples
TM_AFM
10.00 μm
1.598 V
1.174 Hz
512
nrhcvcs.003

(v)

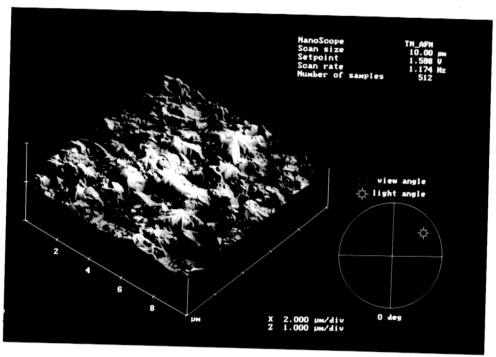
NanoScope
Scan size
Setpoint
Scan rate
Number of samples
TM_AFM
10.00 μm
1.598 V
1.174 Hz
512
view angle
light angle
2
4
6
8
μm
X 2.000 μm/div
Z 1.000 μm/div
0 deg

Fig. 2.28 Profile of HBsAg, anti-HBs, HCVAg and anti-T4 immobilised on WNR surface and PP surface.

(a)HBsAg on PP surface

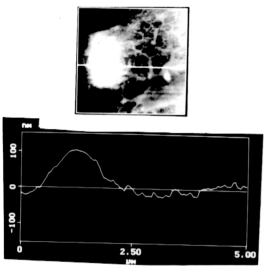


(b) HBsAg on WNR surface

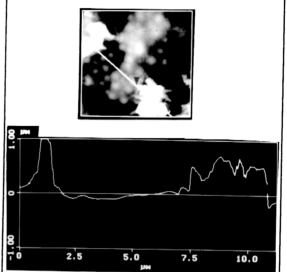


(c) anti-HBs on PP surface

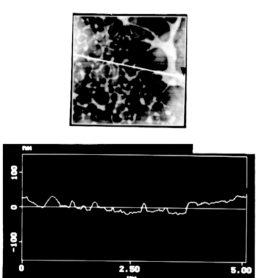


(d) anti-HBs on WNR surface

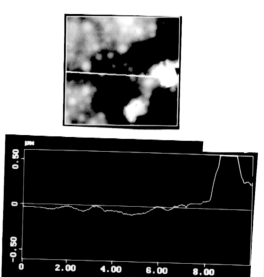

(e) anti-T4 on PP surface

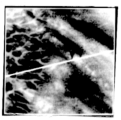

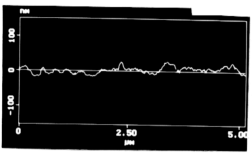


(f) anti-T4 on WNR surface

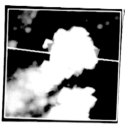

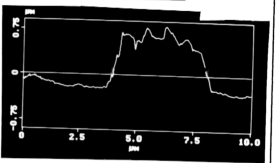


(g) HCV on PP surface

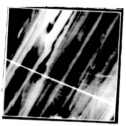

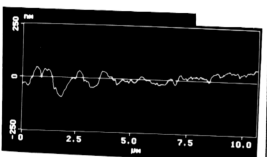


(d) HCVAg on WNR surface

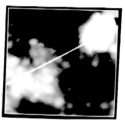

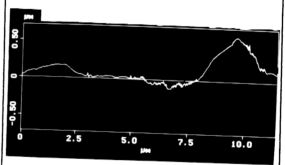

| (i) 50% NBCS on PP surface | (j) 50% NBCS on WNR surface |
| --- | --- |
| 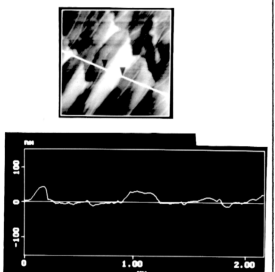  | 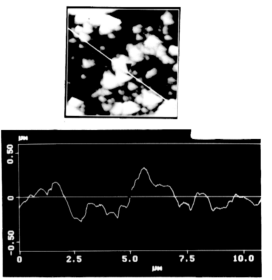  |

## 2.5 Conclusion

A new solid-phase constructed from NR latex film (with PP solid phase as control surface) was formulated for HBsAg, anti-HBs, anti-HCVAg and T4 assays. The study showed that percent binding of proteins was much higher on NR than on PP surface. NR film surface was applicable for both sandwich (HBsAg, anti-HBs, anti-HCVAg assays) and competitive immunoassays (T4 assay), but the sensitivity was rather low as compared to PP as solid phase despite high percent binding of proteins. This was due to high non-specific binding of NR film surface. The adsorption of protein on both PP and NR surfaces was studied using SEM and AFM techniques. Formation of thin layer evenly spread out, dendrite-like aggregates of protein was observed on PP surface. However adsorption of protein on NR surface was in cluster form and submerged into the NR layer. These could possibly be due to (i) difference in hydrophobicity of the two surfaces: PP surface was more hydrophobic thus promoting unfolding of proteins molecules and more even coverage of the surface, whereas the adsorbed antigen-antibody molecules did not unfold on the less hydrophobic NR surface. (ii) NR surface contained inorganic substances and proteins. These may interact with immobilised protein resulting in the formation of aggregates. The high percent binding of anti-HBs/ HBsAg on NR surface was due to clusters formation and not to the uneven NR surface.

In the assay analysis, the low sensitivity of the NR surface are due to (i) substantial denaturation of polyclonal antibodies and antigens passively adsorbed on

NR coated surface. Most of the immobilised antibodies or antigens on NR surface are inactive in their binding properties; (ii) even coating of proteins on PP surface provided larger surface area for interaction between serum antigen or antibody with the immobilised macromolecule. On NR surface, the clusters formed were partially embedded in the natural rubber layer resulting in reduced interaction with the antibodies or antigen;(iii) unfolded proteins on PP surface were tightly adsorbed and could not be displaced by other molecules, whereas added protein could penetrate through NBCS clusters to the NR surface.

**References**


1. Almeida, J.D., A. J. Zuckerma., Taylor, P.E., and Waterson, A. P. (1969) *Microbios.* **2,** 117-123.
2. Arai, T. and Norde,W.(1990) *Colloids Surfaces* **51,** 1.
3. Bayer, M.E., Blumberg B.S., and Werner, B. (1977) *Nature* **218,** 1057-1059.
4. Bernard, A. M., Foidart, J.M, Mahieu, P., Viau.P, and Lauwerys, R.R. (1986) *Clin. Chem.* **32/8,** 1468-1472 .
5. Blumberg, B.S., Gerstley, B. J.S., Hunger Ford, D.A., London, W.T. and Sutnick, A. I.. (1967) *Ann. Intern. Med.* **66,** 924-931.
6. Buijs, J., Lichtenbelr, J. W.Th., Norde, W., Lyklema., J (1995) *Colloids and Surfaces B : Biointerfaces* **5** ,11-23.
7. Bull, H.B. (1956) Adsorption of bovine serum albumin on glass. *Biochem. Biophys. Acta* **19**, 464-471.
8. Burnham, N.A., Dominguez, D., Mowery, R.L., Colton, R.J. (1990) *Phys. Rev. Lett.* **64**, 1931.
9. Bustamante, C., Vesenka, J., Tang, C.L., Ress,W., Guthold, M., Keller, R. (1992) *Biochemistry* **31**, 22.
10. Butler, J.E (1992) The behavior of antigens and antibodies immobilised on solid phase. In " *Structure of Antigens* ", Vol. 1 ( Van Regenmortel, M. H. Vedi ), Chap. 11,. CRC Press, Boca Raton, Florida. p. 208-259.

11. Butler, J.E. (1991) Perspectives, configurations and principles. In *"Immunochemistry of Solid Phase Immunoassay'* (Butler , J.E, edi.), Chap. 1,. CRC Press, Boca Raton, Florida, p3-26.

12. Butler, J.E., Ni , L., Nessler, R., Joshi, K.S., Suter, M., Rosenberg, B., Chang, J., Brown, W.R & Cantarero, C.A. (1992) The physical and fundamental behaviour of capture antibodies adsorbed on PS. *J. Immunol. Methods* **150**, 77-90.

13. Butler.J.E; Ni.Li; Brown. W.R. Joshi. K.S; Ghang.J; Rosenberg. B; Voss. E.W. (1993) *Molecular Immunology*, **30**, 1165-1175.

14. Chairez, R., Steiner, F.B., Melnick, J.L and Dressman , G.R (1973) *Intervirology* **1**, 224-228.

15. Dane, D.S., Cameron, C.H. and Biggs, M. (1970) *Lancet. I* 695-698.

16. Dierks, S. E., Butler, J.E. and Richerson, H.B.(1986) Alter recogniton of surface-adsorbed compared to antigen bound antibodies in ELISA. *Mol. Immunol.* **23**, 403-411.

17. Dill. K. (1990) *Biochemistry* **29,** 7133.

18. Djacadi-Ohaniance, L., Friquet, B. and Goldberg, M.E. (1984) Structural and functional influence of enzyme antibody interactions : Effect of eight different monoclonal antibodies on enzyme activity of Escherichia coli tryptophan synthas. *Biochemistry* **23**, 97-104.

19. Donghao, R.Lu., Kinam, P. (1991) *J .Colloid Interface Science* **144**, 271-281.

20. Elgersma, A.V., Zsom, R.L.J., Norde, W and Lyklema.J (1992) *Colloids & Surfaces* **65,** 17.

21. Eppel, S.J., Zypman, F.R. Marchant, R. E. (1993) *Langmuir* **9**, 2281

22. Feitelson, M ., (1985) The molecular components of Hepatitis B Virus . In : "*Molecular components of Hepatitis B Virus*" (Yechiel. B, edi.), Martinus Nijhoff Publishing, p 2-4.

23. Feng, L., Andeade, J.D. and Hu, C.Z. (1989) Scanning tunnelling microscopy of proteins on graphite surface. *Scanning Microsc.* **3**, 399-410

24. Fields, H. A., Hollinger, F.B,. Desmyter, J., Melnick, J. L and. Dressman, G. R (1977) *Intervirology* **8,** 336-350.

25. Friquet, B., Djavadi-Ohaniance, L. and Goldberg, M.E. (1984) Some monoclonal antibodies raise with a native protein bind preferentially to the denatured antigen. *Mol. Immunol.* **21**, 673.

26. Hansma, P.K., Elings, V.B., Marti, O., Bracker, C.E. (1988) *Science* **242**, 209.

27. Harvey, L.J., Bloomberg. G., Clark, D.C., (1995) *J. Colloid Interface Science* **170**, 161-168.

28. Haynes, C.A., Norde, W. (1994) *Colloids and Surfaces B: Biointerfaces* **2**, 517-566.

29. Haynes, C.A., Norde,W. (1994) Globular proteins at solid/liquid interfaces; *Colloids and Surfaces B : Biointerfaces* **2,** 517-566.

30. Hiroku Kimura, (1980) *J. Immunological Methods* **38**, 353-360

31. Hisrchman, S.Z. (1979) *Biochem.* **26,** 47-67.

32. Ho, C.C. and Khew, M.C. (1996) Proceedings International Rubber Conference, Manchester, U.K, June 1996.

33. Ho, C.C., Subramaniam, A. and Yong. W.M. (1976) *" Lipids associated with particles in Hevea Latex ". Proceedings International Rubber Conference, Kuala Lumpur* **2**, 441.

34. Holland, Z. and Katchalski-Katzir, E. (1986) Use of monoclonal antibodies to detect conformational alterations in the lactate dehydrogenase isoenzyme 5 on heat denaturation and on adsorption to polystyrene plate. *Immunol.* **23**, 927-937.

35. Howard, C. R. and Burrell, C. J.(1976) *Prog. Med. Virol.* **22**, 36-103.

36. Howard, C.R. and A. J. Zuckerman. (1977) *J. Immunol. Methods* **17**, 291-301.

37. Joshi, K.S., Hoffman, L.G. and Butler, J.E. (1992) The immunochemistry of sandwich ELISAs. V. The capture antibody performance of polyclonal antibody-enriched fractions prepared by various methods. *Mol. Immunol.* **23**, 927.

38. Kauzmann, W. (1959) *Adv. Protein Chemistry.* **14**, 1.

39. Kennel, S. (1982) Binding of monoclonal antibody in fluid phase and bound to solid support. *J. Immunol. Methods* **55**, 1.

40. Klotz, S.A., Rutten, J.J., Smith, R.L., Babcock, S.R. and Cunningham, M.D.. (1993) *Microb. Pathog.* **14**, 133.

41. Kochwa, S., Brownell, M., Rosenfield, R.E. and Wasserman, L.R. (1967) Adsorption of proteins by polystyrene particles. I. Molecular unfolding and acquired immunogenicity of IgG. *J. Immunol.* **99**, 981-986.

42. MacRitchi, F. (1972) *J.Colloid Interface Sci.* **38**, 484.

43. Malmsten, M., Lassen, Bo. (1995) *Colloids and Surfaces B: Biointerfaces* **4**, 173-184.

44. Martin, Y., Williams, C.C., Wichramasinghe, H.K. (1987) *J. Appl. Phys.* **61**, 4723.

45. Neurath, A. R., Strick, N. and Oleszko, W. R.(1981) *J. Virol. Methods* **3**, 115-125.

46. Neurath, A.R. and Strick, N. (1982) in *"Viral Hepatitis, 1981 International Symposium"*, (Szmuness, W., Alter, H. J. andMaynard, J.E., edi), Franklin Institute Press, Philadelphia, p. 760-761.

47. Norde, W., Anusiem, A.C.I. (1992) *Colloid & Surfaces* **66**, 73.

48. Norde, W., Favier , J.P. (1992) Structure of adsorbed and desorbed proteins. *Colloids and Surfaces* **64** , 87-93.

49. Norde, Wand Lyklema. J (1991) *J. Biomater. Sci.* **2** 183.

50. Nygren, H. (1988) Experimental demonstration of lateral cohesion in layer of adsorbed protein and in layers of gold antibody complexes bound to surface immobilised antigen. *J. Immunol. Meth.* **114**, 107-114.

51. Nyilas, E., Chiu, T.H. and Herzlinger, G.A. (1974) Thermodynamic of native protein/ foreign surface interactions. I. Colorimetry of the human - globulin/glass system . *Trans Am. Soc. Artif. Intern. Organs* **20**, 480-490.

52. Oscarsson, S. (1994) *J. Colloid Interface Science* **165**, 402-410.

53. Oss, C.J van. (1991) *Biofouling* **4**, 25.

54. Sjollema, J.A., van der Mer, H.C., Uyen, H.M.W., Busscher, H.J. (1990) *J Adhes. Sci. Technol.* **47**, 65.